Kaunas University of Technology

Faculty of Mechanical and Engineering Design

Research and Development of a Body Kit for Passenger Cars to Enhance Aerodynamic Efficiency

Master's Final Degree Project

Richard Stephen

Project author

Assoc. Prof. Dr. Sigitas Kilikevičius

Supervisor

Kaunas, 2021

Kaunas University of Technology

Faculty of Mechanical Engineering and Design

Research and Development of a Body Kit for Passenger Cars to Enhance Aerodynamic Efficiency

Master's Final Degree Project

Vehicle Engineering (6211EX021)

Richard Stephen

Project author

Assoc. Prof. Dr. Sigitas Kilikevičius

Supervisor

Lect. Dr. Kristina Liutkauskienė

Reviewer

Kaunas, 2021

Kaunas University of Technology

Faculty of Mechanical Engineering and Design

Richard Stephen

Research and Development of a Body Kit for Passenger Cars to Enhance Aerodynamic Efficiency

Declaration of Academic Integrity

I confirm the following:

1. I have prepared the final degree project independently and honestly without any violations of the copyrights or other rights of others, following the provisions of the Law on Copyrights and Related Rights of the Republic of Lithuania, the Regulations on the Management and Transfer of Intellectual Property of Kaunas University of Technology (hereinafter – University) and the ethical requirements stipulated by the Code of Academic Ethics of the University.

2. All the data and research results provided in the final degree project are correct and obtained legally; none of the parts of this project are plagiarised from any printed or electronic sources; all the quotations and references provided in the text of the final degree project are indicated in the list of references.

3. I have not paid anyone any monetary funds for the final degree project or the parts thereof unless required by the law.

4. I understand that in the case of any discovery of the fact of dishonesty or violation of any rights of others, the academic penalties will be imposed on me under the procedure applied at the University; I will be expelled from the University and my final degree project can be submitted to the Office of the Ombudsperson for Academic Ethics and Procedures in the examination of a possible violation of academic ethics.

Richard Stephen

Confirmed electronically

Kaunas University of Technology

Faculty of Mechanical Engineering and Design

Study programme: Vehicle Engineering (6211EX021)

Task Assignment of Master's Final Degree Project

Given to the student: Richard Stephen

1. Title of the Project:

Research and Development of a Body Kit for Passenger Cars to Enhance Aerodynamic Efficiency

Kėbulo elementų komplekto lengvųjų automobilių aerodinaminėms savybėms gerinti sukūrimas ir tyrimas

2. Aim of the Project: The main aim of the thesis is to improve aerodynamic vehicular performance for a passenger car by designing aerodynamic features and to investigate the proficiency of the design at different combinations for the respective drag and lift coefficients.

3. Tasks of the Project: Investigate different aerodynamic features of the car, Design of different aerodynamic parts, conduct flow simulation for the stock car to estimate base aerodynamic characteristics, conduct flow simulation on the stock car along with aerodynamic features at different combinations, Comparison of results with the base result obtained.

4. Structure of the Text Part:

- **I.** Introduction
- **II.** Literature Review
- **III.** Methodology
- **IV.** Results and Discussion
- **V.** Conclusion
- **VI.** List of reference

5. Consultants of the Project:

Author of the Final Degree Project Richard Stephen 2020-02-04

(Name, Surname, Date)

Supervisor of the Final Degree Project	Assoc. Prof. Dr. Sigitas Kilikevičius	2020-02-04
	(abbreviation of the position, name, surname, date)	

Head of Study Programme	Prof. Dr. Artūras Keršys	2020-02-04
	(abbreviation of the position, name, surname, date)	

Stephen, Richard. Research and Development of a Body Kit for Passenger Cars to Enhance Aerodynamic Efficiency. Master's Final Degree Project / supervisor Assoc. Prof. Dr. Sigitas Kilikevičius; Faculty of Mechanical Engineering and Design, Kaunas University of Technology.

Study field and area (study field group): Transport Engineering (E12), Engineering Science.

Keywords: Spoiler, Diffuser, Side skirt, Splitter, CFD Analysis, Solidworks, Inclination angle, Drag coefficient, Lift coefficient

Kaunas, 75 p.

Summary

The primary purpose of this project is to improve the aerodynamic performance of a passenger car. This is accomplished by attaching different aerodynamic features to the stock car. Mazda CX-9 2020 is the model chosen, and designed as per the dimensions of the manufacturer. Solidworks 2019 is the software used to design the aerodynamic features and the CFD flow simulation is performed using the same. Primarily, the base model is analyzed and the results procured is set as the base results for comparision. Individual analysis of the diffuser and side skirt is performed to identify the optimum drag and lift coefficients for the car, which is then used in the configuration as the standard angle and height respectively. The study is improved by analyzing aerodynamic characteristics of the stock car along with different combinations of aerodynamic features and angle of spoiler inclination. The result obtained is collated with that of the base results and the best combinations of the parts with aerodynamic characteristic is chosen. The influence of aerodynamic properties together with the combination of various elements additionally mounted to the car has been determined.

Stephen, Richard. Kėbulo elementų komplekto lengvųjų automobilių aerodinaminėms savybėms gerinti sukūrimas ir tyrimas. Magistro baigiamasis projektas / vadovas doc. Sigitas Kilikevičius; Mechanikos inžinerijos ir dizaino fakultetas. Kauno technologijos universitetas.

Studijų kryptis ir sritis (studijų krypčių grupė): Transporto inžinerija (E12), Inžinerijos mokslai.

Reikšminiai žodžiai: Spoileris, difuzorius, šoninis sijonas, skirstytuvas, CFD analizė, Solidworks, pasvirimo kampas, tempimo koeficientas, kėlimo koeficientas

Kaunas, 2021. 75 p.

Santrauka

Pagrindinis magistro baigiamojo projekto tikslas yra pagerinti aerodinamines keleivinio automobilio savybes. Šis patobulinimas buvo įgyvendintas pritvirtinus įvairius aerodinamikos savybes pagerinančius elementus prie serijinio automobilio. Magistro baigiamajame projekte kaip bazinis, buvo pasirinktas Mazda CX-9 2020 automobilis, kurio erdvinis modelis buvo sudarytas pagal gamintojų pateiktus matmenis. Projektuojant kėbulo elementų komplektą ir atliekant aerodinaminį oro aptekėjimo modeliavimą, buvo panaudota SolidWorks 2019 programinė įranga. Pirmiausia, yra atliekama bazinio modelio analizė, o gauti skaičiavimo rezultatai priimami už etaloną. Taip pat, yra atliekama individualaus difuzoriaus ir šoninio automobilio slenksčio analizė, kurios metu siekiama nustatyti optimalų automobilio pasipriešinimo ir keliamosios jėgos koeficientą, kuris toliau yra panaudojamas sudarant elementų aukščių ir montavimo kampų konfigūracijas. Magistro baigiamajame projekte ištirtos serijinio automobilio ir pagalbinių kėbulo elementų aerodinaminės charakteristikos, kartu su aptako pasvirimo kampų kombinacijomis, bei nustatyta kokią įtaką automobilio aerodinaminėms savybėms daro papildomai montuojamų įvairų elementų kombinacijos. Gauti rezultatai buvo palyginti su gautomis etaloninėmis reikšmėmis ir buvo parinkta geriausia automobilio komplekto aerodinaminių elementų kombinacija su geriausiomis aerodinaminėmis savybėmis.

Table of Content

List of Figures

List of Tables

Introduction

When it comes to aerodynamics of vehicles, air is considered a fluid and its main purpose is to reduce drag, wind noise and preventing undesired lift force and other factors that cause aerodynamic instability of the car at high speeds. Performance and consumption of fuel play a major role in the aerodynamics of a car. A vehicle with low drag coefficient is bound to have better fuel efficiency when compared to a car which is less aerodynamically optimized.

Though the origin of aerodynamics of road vehicles was from the aerodynamics of aircrafts, they do still differ in several ways. Firstly, the body shape of the car is much less streamlined in comparison to that of an aircraft. Second, cars operate much closer to the ground while the aircrafts operate in free air. Third, aerodynamic drag depends on the speed of the moving object and the speeds at which the aircrafts travel is much higher than the road cars, thus varying drag. Fourth, the aircraft travelling in free air have more degrees of freedom than a car travelling on the road with lesser degrees of freedom. Fifth, the vehicles be it aircrafts in free space or cars on road, they are designed depending on their purpose. The most important issues that the Automotive industry faces today is to reduce emissions and fuel consumption. There are many sectors in which improvements on a car can be done to reduce fuel consumption such as improving the engine efficiency and aerodynamics of the vehicle.

Aim of the project

This thesis aims to enhance aerodynamic vehicular performance for a passenger car by designing aerodynamic features and to investigate the proficiency of the design at different combinations for the respective drag and lift coefficients.

Tasks to reach aim of the project:

1. Investigate different aerodynamic features of the car along with various techniques used for flow simulation.
2. Design of different aerodynamic parts with all dimensions based on the governing body
3. Conducting flow simulation for the stock car to estimate base aerodynamic characteristics, namely lift coefficient, lift force, drag coefficient, and drag force.
4. Conduct flow simulation on the stock car along with seven different combinations of aerodynamic features also called configurations at different angles of spoiler inclination.
5. Comparison of results acquired with the base model result to determine the prime configuration that produces the prime aerodynamic properties.

1. Literature review

The review about various studies and different experiments using aerodynamic devices that have been performed over the years to enhance the aerodynamic parameters are done in this section. This segment is split into three parts:

1.1. History of aerodynamics

The chronicles of aerodynamics in automobile takes place in four indistinct phases. As the driving speeds increased, the sensitivity to cross winds rose along with it. By suitably shaping the body of car, attempts were made to eliminate the deposition of water and dirt on the lights and windows. In the 19thcentury tests on vehicles for drag coefficients were done through coast down tests or by measuring the maximum speed of the vehicle, both of which led to errors. The history of aerodynamics in automobile accounts for two aims. Firstly, the work which contributed for the development in automobile aerodynamics. Secondly, the application of this obtained knowledge in the automobile design.

In the early 19th century attempts were made to make the automobile as streamlined as possible with designs obtained from the disciples of naval and airship engineering. The aerodynamic drag played a very subordinate role for the reasons being low engine power, speeds, and poor road conditions. According to the aerodynamic principles the oldest vehicle built was the one by Camille Jenatzy which was electrically driven and exceeded speeds of 100 Km/h. Its shape was of a torpedo and the body was streamlined, but the wheels and the driver were not integrated which later led to an increase in drag.

After the First world war, the “Rumpler-Taube” was designed in the shape of a teardrop. When viewed from the top, the vehicle was shaped as an Aerofoil and the roof was well streamlined. The car designed by Rumpler had the wheels uncovered and hence led to increase in drag. Later Jaray a pioneer in automotive streamlining designed the vehicle using sections from bodies called as half bodies. This form of design of the vehicle was later called as combination form. With this technique low drag was achieved as the separation of air flow at the rear was eliminated. This could be achieved as a long tail called ‘slender tail’ was integrated into the rear of the car. This design was later incorporated with a well-rounded front and was called ‘Lange car’.

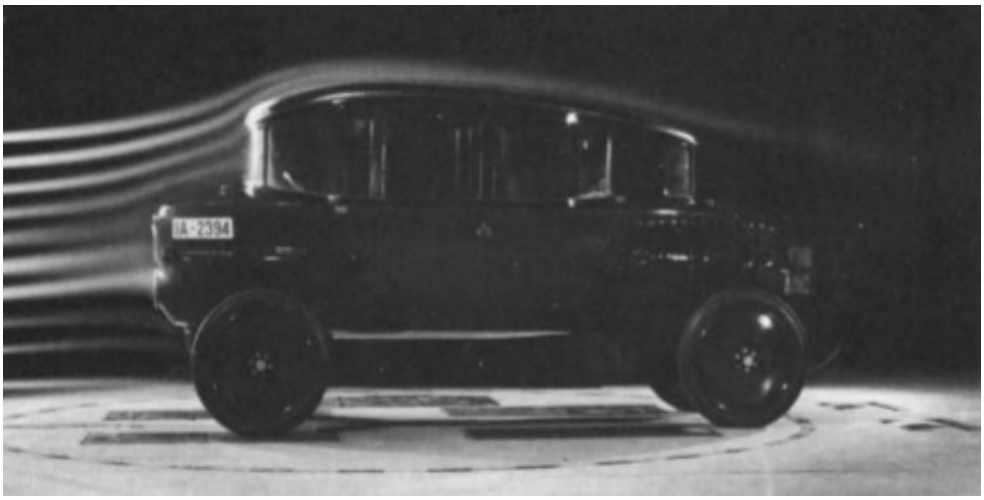

Fig. 1. Rumpler Car [12]

A scientist, Lay modified the shape of the car at the front and the rear end symmetrically and isolated the aerodynamic effects. Investigations revealed that there were strong interactions between the flow fields of the front and the rear end of the car. As the flow of air was well attached along the front of the car, low drag for a long-tailed model car was well maintained. But as the flow separated at the steep windshield the drag drastically increased. This design was a failure and could not be built due to the increase in drag. The important results obtained from Lay's work was that a blunt rear end had slight increase in drag in comparison to that of a long-tapered end. The works of Lay was then improvised my Kamm and this led to the introduction of 'Kamm-back' cars. These cars had a blunt rear end as that of the cars designed by Lay and low drag was achieved as the flow of air remained attached as long as possible. The car's body was tapered and the pressure at the rear end of the car was increased which reduced the overall drag.

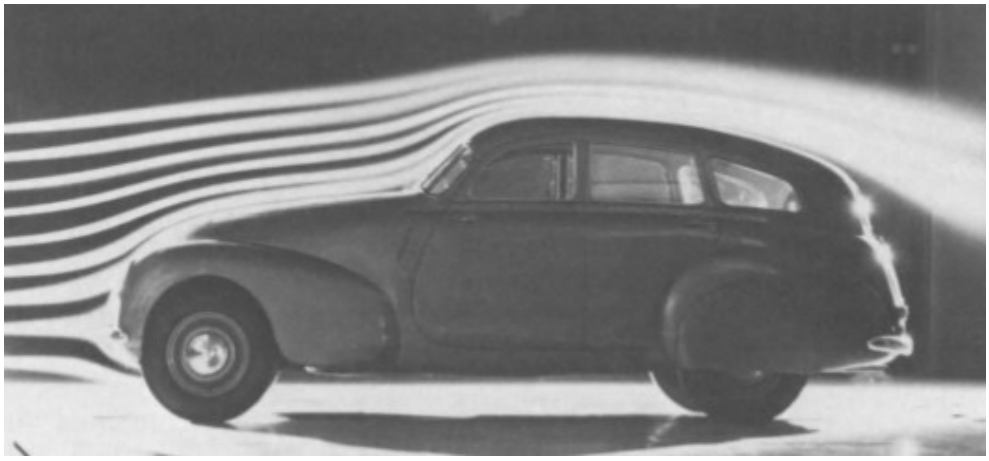

Fig. 2. Kamm Car [12]

As further improvements were made with drag, directional stability with respect to cross winds became significant with greater speeds. It was later discovered that vehicles with low drag and

long tapering ends possessed lower stability with cross winds. Klemperer a German scientist prominent in the field of aviation took into consideration the flow of air through the cooling system. The results obtained showed that the flow of air through the radiator increased drag.

In order to reduce drag further, optimization technique was initiated. The method was developed by Hucho, Janssen and Emmelmann. In the technique the shape of the car was optimized such as the curvature, spoiler, taper, radii, etc. were modified in combination, sequence or step by step to reduce the separation and to control the air flow separation resulting in reduced drag. The development of the aerodynamics of the car can also be started with a body of low drag with the exact overall dimensions of the final car. This configuration is then converted into the real car by the application of optimization technique step by step.

As seen from the early 19th century developments in the sector of aerodynamics for automobile has progressed and improvements in the field are being carried out. In terms of technology such as wind tunnels being used by different companies to improve the performance of their car. The field of aerodynamics achieves its peak in motorsports [12].

Fig. 3. Optimization of body details [10]

1.2. Aerodynamic parameters

One of the ways to achieve high performance of cars is by improving the aerodynamic parameters. The most important parameters of aerodynamics include drag, coefficient of drag, lift, coefficient of lift, drag force and downforce.

1.2.1. Downforce

Downforce as the name suggests is a force that pushes the car downward to the road making the tires stick to the ground to provide better traction, it is also called negative lift. Downforce increases as the distance between base plate of the car and the ground decreases. It is because as

the distance between base plate of the car and the ground decreases the velocity of air flowing underneath the car increases and a low-pressure region is created. The low-pressure region causes a suction force to be created underneath the car, downforce decreases as the distance between the plate and ground increase.

1.2.2. Lift

Lift is crucial for cars travelling at high speeds. It is the force that is acting in opposition to the weight of the vehicle. As the lift of the car increases the car tends to behave like a wing and slowly loses contact with the ground. As the air on the top of the car is at a lower pressure when compared to the air on the bottom, difference in pressure is created and the pressure on the top surface of the car decreases. The force acting on the bottom of the car is greater than the force acting on top of the car. This reduces the amount of load acting on the wheels of the car which in turn reduces the traction of the wheels to the road, hence causing lift.

The equation for Lift force:

$$L = \frac{CI*\rho*v^2*A}{2}; \quad (1.1)$$

The coefficient of lift is a dimensionless quantity, the lift that is generated by a lifting body to the fluid velocity, fluid density around the body and the associated reference area of the lifting body.

The equation for coefficient of Lift force:

$$C_L = \frac{2L}{\rho*v^2*A}; \quad (1.2)$$

where:

L - Lift force;
ρ - Density of the air;
V - Velocity of the air;
A - Frontal area.

1.2.3. Drag

Drag is the force which is generated when the motion of the body is resisted. The drag of a car depends on the frontal area of the vehicle. Vehicles which have a larger frontal area are subjected to more pressure drag compared to streamline bodies. Drag forces acting on a car can be split into four types, that is induced drag, interference drag, viscous drag and separation pressure drag.

Induced drag is generated when lift or downforce is created, that is when there is a pressure difference between the surfaces of the car. When the air flows over other parts of the car such as its body section interference drag is created. For instance, the air flow over the bonnet will be

affected by the air coming off at the nose of the car. Viscosity is the property of the fluid by which it shows resistance to deformation at a given rate. The drag created by air to the flow over the surface of the car is viscous drag. Separation pressure drag is the drag which is created with the separation of the flow of air. It primarily depends on the laminar flow and turbulent flow of air. The drag created by this separation is separation pressure drag.

The equation of Drag force:

$$D = \frac{Cd*\rho*v^2*A}{2}; \quad (1.3)$$

The coefficient of drag is also a dimensionless quantity.

The equation for coefficient of Drag force:

$$C_D = \frac{2D}{\rho*v^2*A}; \quad (1.4)$$

where:

D - Drag force;
ρ - Density of air;
V - Velocity of the air;
A - frontal area of car.

1.3. Aerodynamic devices

There are various aerodynamic devices such as the spoiler or inverted wing, splitters, diffusers, canards, side skirts, vortex generators that helps in manipulating the flow of air around the body of the car to achieve the desired results.

1.3.1. Inverted Aerofoil

Primarily inverted wings create downforce due to pressure difference that take place at the top and bottom surface of the designed wing. The flow of air about the inverted wing is such that some of the air flows over the top of the wing and the rest travels on the bottom surface of the wing. Depending on the design of the wing, the air that flows on the top surface moves slow creating a region of high pressure and the air flowing under the wing moves at a higher velocity creating a region of low pressure. This pressure difference is such that it causes the top surface to push the vehicle down with a greater force when compared to that of the lower surface pushing up, thus creating more down force. The rear wing's design, position and the Inclination angle plays a vital role in how the air flows and in turn affecting the attributes of vehicle aerodynamics. An adaptive rear wing creates small vortices which requires lesser energy to be generated and hence lesser drag.

Fig. 4. Aerofoil of a car [10]

1.3.2. Air dams

Air dam limits the flow of air going under the car. This device forces the air around and over the car resulting in an increase in air pressure at this region. The volume of air that passes under the car travels faster creating a low-pressure region and resulting in suction effect.

1.3.3. Splitter

Splitter as the name suggests, it splits the flow of air coming on to the car. The splitter functions on the same principal as that of an air dam. Since the front of the car is blunt, high-pressure region is created by the air that is pushed against the surface of the car and slowing it at the same time. The splitter splits this region into high pressure and low-pressure regions and simultaneously increasing down force.

Fig. 5. Airflow by the Splitter [9]

1.3.4. Diffuser

Diffuser is a device that reduces the pressure on the lower end of the car. It is generally located just below the splitter to direct the air into the front wheel wells and under the car. The rear diffuser pushes the air from under the car into the turbulent wake region. The underbody diffuser includes three mechanisms upsweep, ground interaction and diffuser pumping. By increasing the angle of

the diffuser, the down force can be increased and vice versa. The ground clearance of the car also plays a crucial role, as the ride height of the car decreases down force increases.

Fig. 6. Diffuser on a Nissan Skyline [9]

1.3.5. Canards

Canards also called drive plates is another device used to generate down force as they direct the flow of air in the upward direction and creating downward force. Canards create strong vortices that move along the sides of the vehicle which prevents the high-pressure air from interfering with the air flow of the low-pressure region underneath the car. Canards have a downside, that is on addition of this device a lot of drag is created. So, to curb this increase in drag fine tuning of aerodynamic devices is required.

Fig. 7. Airflow through the Canards [9]

1.3.6. Side skirts

Side skirts is a device that helps in controlling the amount of air that flows under the car. The effectiveness of the side skirts depends on the ground clearance of the vehicle. If the height of the side skirt is above a certain level its effectiveness decreases. The side skirts also separate the flow of air into high pressure and low-pressure regions.

Fig. 8. Airflow pattern through the side ducts [9]

1.4. Methods of investigation

The behavior of flow of air under a vehicle was in a different manner when the distance between the lower end of the car and the ground was under proximity. The primary objective of this research was to increase the downforce by accelerating the air flow on the underside of the car and reducing the cross-sectional area to create an area of low pressure. The investigation was performed on an airfoil. Computational Fluid Dynamics is utilized to perform boundary layer suction and compared with XFOIL suction to predict the drag and downforce of race cars travelling at high velocities. Since the wings of racecars are made of multiple layers the boundary layer technique which is used identifies that a small layer of air above the wing can be removed and has an effect of stabilizing the postponing transition and separation. By means of this technique low drag and high lift forces can be achieved [1].

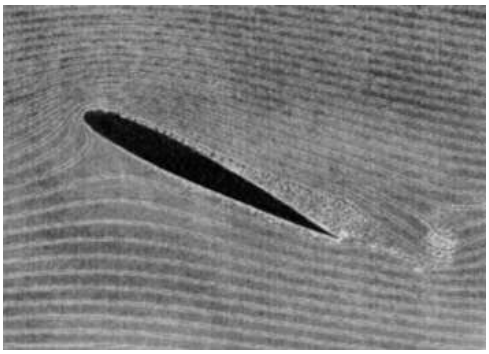

Fig. 9. Rear wing of racecar subjected to Boundary layer suction technique [1]

The investigation and design of active aerodynamic surfaces in a closed loop system is the focus. These active aerodynamic surfaces are moved by using servo mechanism. The active aerodynamic surfaces are designed for the optimization of comfort without being affected by road conditions and the coordination of semi active or passive suspensions. The Inclination angle on the rear wing plays a vital role in the comfort. So, depending on the speed and frequency of the vehicle, the rear wing adjusts itself with respect to the speed it is moving and hence provide better ride comfort.

The research about the rear wing working in hand with the suspension system that is either active or passive suspension system signifies how the ride of the vehicle is advanced irrespective of the road conditions [2].

The rear wing and other aerodynamic devices are important as they significantly affect the drag coefficient of a car. Investigation on down force is performed as attachment of aerodynamic devices significantly affects the down force as it provides more traction to the ground. The study is investigated in three-dimensional CFDa simulation by using Autodesk Software. The simulation is carried out with 5 different velocities. The results obtained clearly state that, with the help of an aerodynamic device such as the rear wing drag drastically reduces when compared to the drag coefficient of a vehicle without a rear wing [3].

This research is based on the investigation of aerodynamic devices on a race car. The center of racing design revolves around drag and fuel efficiency. When greater amounts of downforce are generated more drag is also created but the average speed improves on the circuit. Detailed investigation on the aerodynamic devices such as inverted wing, diffuser, front splitter, vortex generator is performed. The height between the road and the under surface of the car is reduced and suction is created which provides more traction to the car [4].

A duct is created from the front of the car to the rear end. As the main cause of drag is the low-pressure region called the wake region that is created on the rear end of the car. By creating this duct from the front of the car to the rear the drag is reduced which simultaneously improves fuel efficiency. The three-dimensional modelling of the vehicle is designed in PRO E software. Analysis is performed in Ansys for different rear angles of inclination from 0 to 13. Thus, based on the analysis performed the drag was comparatively lower obtained after the duct was created [5].

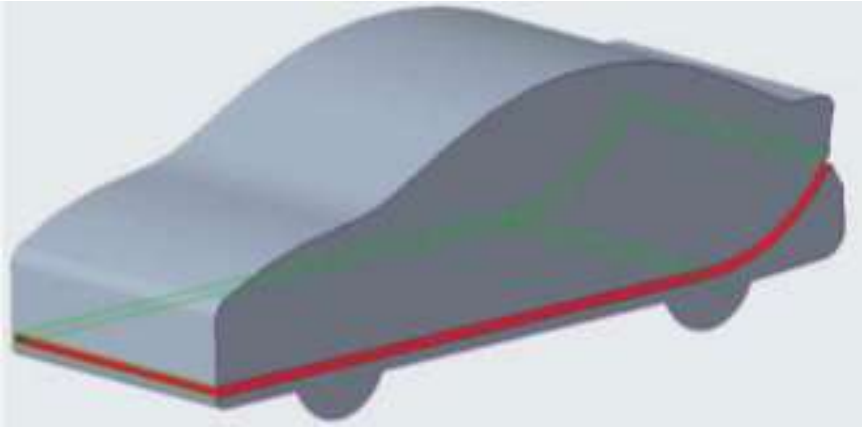

Fig. 10. Car model designed in PRO E [5]

Improving the aerodynamic drag of a car by means of a diffuser which will improve pressure recovery on the underbody of the car. Computational Fluid Dynamic simulation is used to perform analysis on the diffuser. Two-dimensional finite element test using CFD is performed on the

diffuser at 6 different angles ranging from 0 degree to 15 degree. The results obtained show that drag is influenced by rear diffuser angles. As the rear diffuser angle increases the mass of air flow on the underbody is increased. This causes the velocity of air to increase in turn reducing the drag force of the car [6].

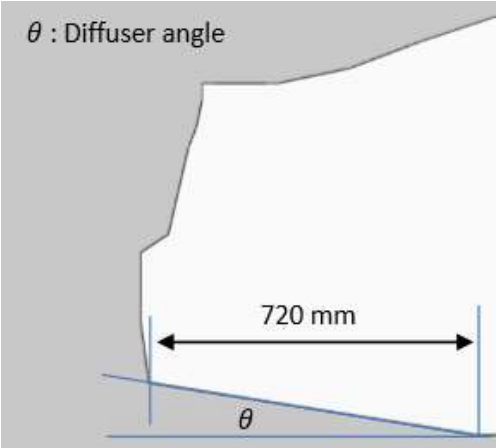

Fig. 11. Configuration of Diffuser angle [6]

The utilization of negative lift greatly impacts the performance of the race car. Various methods such as the use of inverted wings, a diffuser and a vortex generator are investigated. With the introduction of these aerodynamic devices, significant results are noticed with the flow boundary layer transition. Wind tunnel testing, track testing, computational fluid dynamics and the research related to the tests mentioned are also investigated. The study performed is in comparison with that of the airplanes and more emphasis are given to the principles of downforce as it plays a major role in the performance of race cars especially at the high-speed corners. With the effects of boundary layer transition, flow separation, and vortex flows, the prediction of the flow of air around the race cars becomes tedious [7].

This study focuses on the wing of a car operating in the wake region. The wing is analyzed in the freestream and ground effects. In terms of ground effect, the downforce depends on the length of the wing. The model is designed in Solidworks and analysis is performed using Ansys. Greater downforce allows the car to turn at high speed in the corners. With the attachment of aerodynamic devices, the race car exhibits variations in acceleration, deceleration, and cornering speeds as they determine how fast the car travels in a circuit. Changes in the wing velocity, angle of attack and ground clearance indirectly influences the aerodynamics of the vehicle. With the addition of these devices in relation with the ground clearance the wake region is also affected [8].

The analysis of aerodynamic attributes of a motor vehicle determines the behavior of various surface features with respect to drag force. Using surface modelling technique, a scaled model of Mercedes-Benz SLS AMG is designed in a software Creo 2.0 which is then modified to reduce

drag force. The model is analyzed with Computational Fluid Dynamics (CFD) software to determine the drag coefficients of both the scaled original design and the modified model, the results are then compared. The modified scale model possesses vents to direct the air flow from the front and sides of the vehicle. A three-dimensional model is printed, and the model is tested in a wind tunnel. The main purpose of the 3-D model was to compare the results of the ones obtained in software analysis with the ones obtained from the wind tunnel test. The results obtained indicate that the drag coefficient of the modified car is less when compared to the original scale model [9].

In this research the car is designed using Autodesk 3ds Max. To design the car efficiently polygonal method of modeling is used to represent a better conceptual design. The digital images are generated once all the modeling of the car is completed. The digital image that was previously generated using Metal Ray rendering which is by default a tool in Autodesk 3ds Max. More focus is given to the exterior design of the car. Using Ansys Fluent a 2D simulation is performed on the designed model and the model is analyzed. The purpose of the analysis is to bring changes in the geometry of the model, to improve design and the aerodynamics of the car. Design is given more importance to the angle between the hood and the front windshield. Analysis of the designed car with a rear wing and without a rear wing is also carried out. From the results obtained the car is modified for better aerodynamic properties. Once again, the modified car goes through simulation and analysis and the results of the original car and the modified car is assessed [10].

At high speeds, the velocity between the oncoming wind and the side winds is high. The wind at high velocities induces high stress on the bumper. The bumper may undergo deformation due the stresses caused by the wind. The functionality of the bumper may be hampered if the deformation exceeds the predesigned value. Wind induced stress analysis is performed on the bumper to quantify the nature and effect of these stresses. The modeling is executed in Creo 2.2 and the structural analysis and CFD simulation is put through Ansys Workbench. The results attained for the structural and fluid flow analysis for the deformation and induced stress values are summarized [11].

This analytical research is based on the performance of the National Association of Stock Car Auto Racing (NASCAR) COT (car of tomorrow) with the rear wing and a spoiler. The yaw angle between 0° and 180° cases are taken, tests are carried out using velocimetry to study the flow pattern differences of the aerodynamic devices generating downforce. Investigation on the zero-degree yaw is performed and observations were made such that the wake which is generated by the wing in comparison to the wake generated by the spoiler is safer for competitive racing in terms of handling. At 180° yaw it is noticed that the wake generated causes improper functioning of the anti-flipping devices also called roof flaps on the winged cars. In extreme degrees of yaw, the flow scales are investigated, and it is observed that the wing has a stronger dependency on Reynolds number (Re) [13]. At a certain height, the spoiler with small angle of attack produces high drag forces. Since the angle of attack is small, it will create small recirculation zones at the back end of the running vehicle. This causes a pressure difference in the regions in front and behind the spoiler thereby increasing the downforce. Out of the six different simulations 12° angle of attack was the

optimum as small increase in drag of 1.56% was detected and the coefficient of lift remained minimum [27].

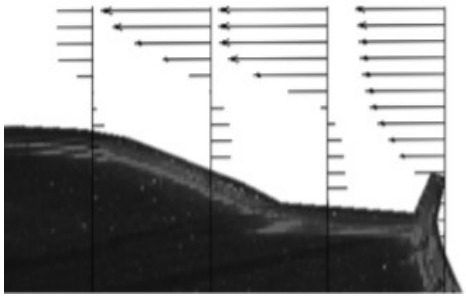

Fig. 12. Velocity profile of a spoiler [13]

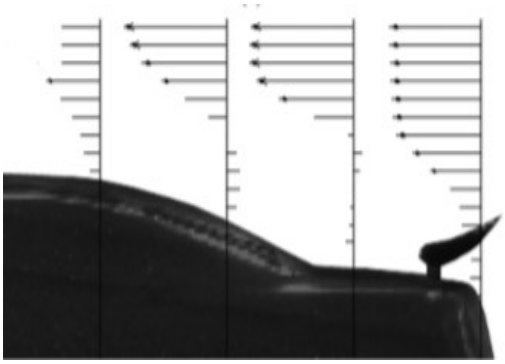

Fig. 13. Velocity profile of a wing [13]

CFD simulation for a transient air flow in a two-dimensional cylinder is performed additionally a spoiler design with six different vehicle models is compared. In this study K – epsilon turbulence model is used in the aerodynamic simulation and LES turbulence model is used for aero-acoustics. A twostep methodology was used to validate and develop the Mach number. This method is resourceful and has better accuracy. The test run is for unsteady turbulent modeling, the results obtained are less accurate. A study of the effect of wind on the car with and without the spoiler is done. It was perceived that with the angle of attack of the spoiler the aerodynamic coefficient of lift reduces [16].

In this study results are obtained from active spoiler. With the movement of the spoiler at 55 degree a downforce equal to a rear wing with an angle of 15 degree is obtained, that is with change in the angle of attack of the spoiler significant downforce is generated. A scaled car model of 1:2.5 ratio is fitted with moving surfaces. This model is tested in the wind tunnel and the aerodynamic coefficients were determined. In the wind tunnel the aerodynamic properties are measured at different angles of wing and spoiler. The flow separation showed that SST and SST k-ω and for r-k-ε and k-kl-ω the separation of flow was limited [17].

Fig. 14. 1:2.5 scale model of the car [17]

A study was performed on the NASCAR to influence the drag on a trailing vehicle. By using the blown ducts, reduction in drag appears through a range of vehicle spacing. It is easier to reduce the drag if the spacing is about 0.25 and 1.00 vehicle length. The exit angle when kept perpendicular to the distance of travel, there is reduction in trailing drag. The results show that 0.5 to 1.0 vehicle distance is the result obtained after validation. With this result which was obtained using Kiel probe measurements in the wind tunnel and anecdotal analysis supports that there is a reduction in drag for the trailing vehicle [18].

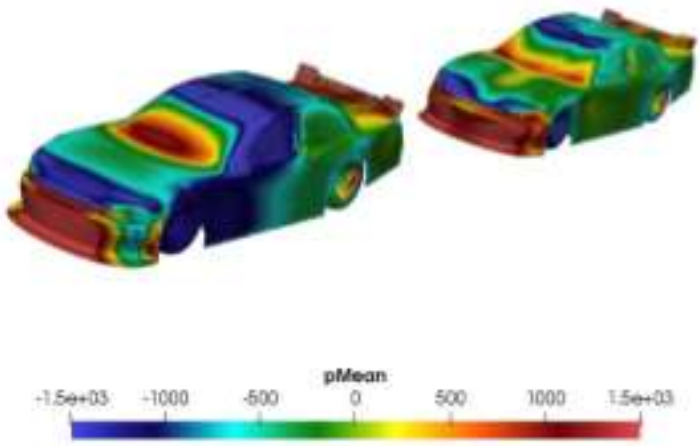

Fig. 15. Leading and trailing vehicle pressure distribution [18]

The CFX method in Ansys is incorporated for simulation of a car with the spoiler and without the spoiler. There are two types of mesh being used the solution is obtained using the RANS equation. There are two models on which the RANS equation is applied K-epsilon turbulence model and the K-Omega turbulence model. For different size and type of mesh for simulation different results are acquired. The results from the K-Omega method are such that the fluid flows smooth and thus reduces the swirls that are created at the rear of the car. The coefficients of drag and lift which are

solved using equations are larger when compared to the K-Epsilon method. In K-Omega method the downforce generated is higher than the K-epsilon method, but the drag created is also high [25].

In this research the car is designed using PRO-E 5.0, the analysis of the model is executed in Fluent – Ansys. The purpose being drag reduction, by improving the aerodynamic parameters of the car using CFD. Analysis of the aerodynamic parameters of the car in a turbulent environment is implemented using CFD and experimental calculations are also performed. The results of drag coefficients achieved using experimentally and software simulation were tabulated and was varied by 0.243 [21].

The objective is to understand how the diffuser performs and how it is advantageous in reducing the drag and lift coefficients of the vehicle. Computational Fluid Dynamics is used for the determination of maximum downforce at the optimum angle of the diffuser. Ansys 14.0 is used for the analysis of drag and lift coefficients. With the addition of the diffuser the results show that the there is a minimal increase in drag and hence does not have a great effect. At 7° of diffuser angle there was an improvement of 1.3-1.4% in drag reduction. At angles of 8° and 40 m/s maximum downforce of -0.305947 was obtained. Thus, downforce increases as the speed of the vehicle increases due to increase in pressure on the upper surface of the vehicle [22]. Similarly, research shows for diffuser angles set were to 0°, 3°, 6°, 9.8°, 12°, with the angle of 9.8° being the original model. It was perceived that as the angle of the diffuser increases the wake and the pressure changes. Thus, the total drag coefficient initially decreases and later increases while the lift coefficient decreases [24].

In this work open road setup is used in comparison to simulation of the vehicle in wind tunnel. A sedan type of vehicle is simulated under different configurations and the results obtained from the simulation is compared with the results of the physical test. It was seen that the drag prediction was adequate as the results of the wind tunnel were compared to the uncorrected data from the wind tunnel. Though the drag prediction was adequate the lift was unsatisfactory [23].

The scope of this article is to design a prototype to achieve better fuel efficiency. To develop a vehicle for better fuel efficiency Computational Fluid Dynamic analysis using Ansys is conducted in order to improve the geometry and overall drag force. Lift was evaluated for stability and boundary layer parameters for drag reduction. From the results, the airfoil shape is preferable for better drag reduction. In order to overcome the dimension issues Kamm back shape was used. Spoiler was added to the rear, but it was not beneficial since the overall drag increased [26].

CFD analysis for a production car is performed. The results derived from the simulation matched that of the predefined values of the car. Additionally, modifications were done by adding a diffuser at the rear end of the car. Initial drag coefficient being 0.3649, the diffuser angle 8° reduced the lift coefficient by 34% and 0.5% increase in coefficient of drag. With further increase in diffuser angle 10° and 15° the lift coefficient further decreased but the coefficient of drag increased. With

the addition of spoiler to the previous setup the lift characteristic improved and there was negligible improvement in drag [28].

The streamlined loads following up on the fast vehicles, play a critical role in terms of design optimization. In this investigation, the fundamental objective is to explore the impact of the limit conditions at the ground level of primary streamlined quality of an open-wheel race vehicle utilizing the resources such as CFD, CFX [29]. The impact of the ground on the primary streamlined attributes of the vehicle, drag and lift, is concentrated in two different ways, the first being the wind tunnel with negligible effect on the ground, and the second being an approach that uses a moving wall. The end results are exhibited by the outcomes, utilizing the general increment of pitching moment, drag, and lift, by the designs visualizations. Introduction of contemplations concerning the significance of the pivoting wheels in optimal design of the street vehicle and the freedom to reenact it in a virtual climate.

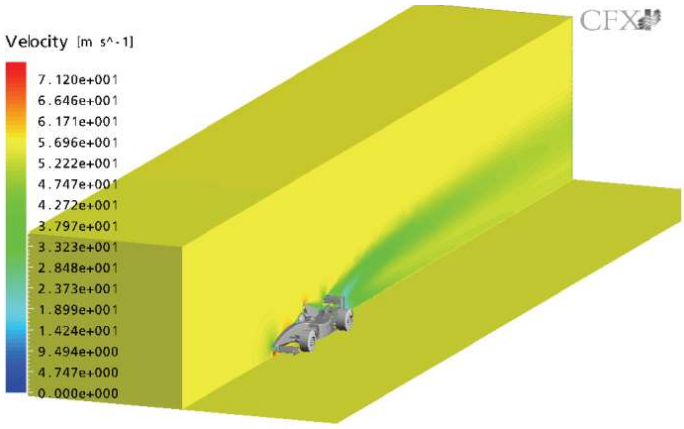

Fig. 16. Visualization of velocity contours in the computational domain [29]

In this paper, ANSYS CFX strategy is utilized to enforce a model attached with a spoiler and without it, by using two different kinds of mesh. The arrangement of the Reynolds Average Navier Stokes equation (RANS equation) has been achieved by utilizing two models, K-Epsilon and K – Omega Turbulence model [30]. Here the mesh size, turbulence, boundary condition simulation has been completely investigated and result for the models has likewise been analyzed. ANSYS programming was utilized to derive the lift and drag powers at different motor energy factors k-Epsilon and K-Omega for the given vehicle area.

The mathematical reproduction and wind tunnel are utilized to examine the streamlined attributes of car. In this article research on streamlined parameters for on underbody of the car is carried out. In the air stream, the drag of the car is rearranged at the same level as the underbody. At that point the mathematical computation model with genuine underbody structure is set up on this premise. Computation results show that there are numerous partition vortexes in the underbody. With an incredible impact on the streamlined attributes, the formation of streamlined drag shoots by 23.4 %. To decrease drag, A wheel spoiler along with three types of underbody spoiler are designed,

and the impact of the vital boundaries on streamlined drag is investigated. Results exhibit both had a successful impact for lessening drag, and the biggest drop of drag coefficient are 4.86 % and 7.05 % [31].

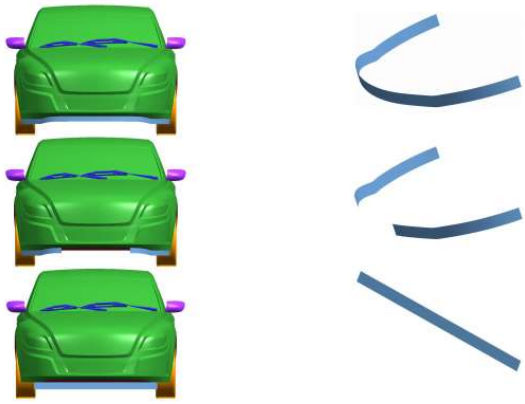

Fig. 17. Underbody spoiler investigates for three different scenarios [31]

When performing mathematical simulation for cars, the space utilized is frequently a huge box with an extremely low blockage proportion and a completely moving ground plane, duplicating open street conditions. Notwithstanding, the actual estimations to which the recreation results are normally looked, with inadequacies concerning blockage, ground displaying, and other limit impedance impacts [32]. A portion of these impacts are adjusted, yet remedies are typically performed on a worldwide level and subsequently neglect to address for neighborhood impacts that may impact various arrangements of the vehicle in various ways. In this work, the ordinary open street mathematical arrangement is contrasted with reproductions where the computational space is a virtual model of the total opened divider air stream test area. The outcomes show that the total drag coefficient can be anticipated with excellent accuracy by simulating the vehicle inside the air stream whenever contrasted with on inaccurate data.

A scientific examination on wind impacts on the PACE Formula 1 race vehicle is introduced. The examination fuses Computational Fluid Dynamic investigation and recreation to increase down force and limit drag during high-speed movement of the race car. Utilizing Star CCM+ programming, the simulation uses productive lattice methods and practical stacking conditions to comprehend downforce on front and back wing parts of the vehicle just as drag made by every external surface. Wing and external surface stacking under high-speed runs of the vehicle are outlined. Enhancement of wing directions (direct approach) and mathematical alterations on external surfaces of the vehicle are performed to improve downforce and reduce drag for greatest stability and control during performance. The CFD analysis calls attention to the current front and back wings, as the car does not produce the ideal downforce and that the back wing ought to be overhauled for better performance [33].

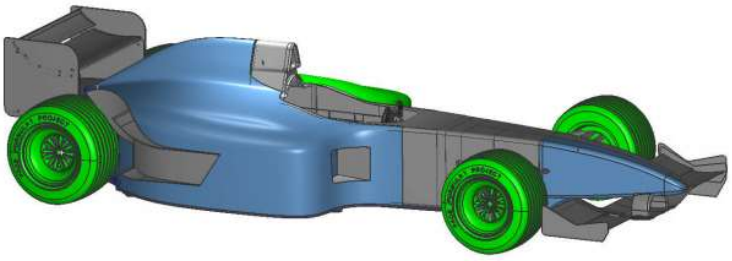

Fig. 18. Designed CAD model of the car with corrections [33]

The paper proposes an investigation of a GT2 with a computational fluid dynamics (CFD) instrument. Results of STAR-CCM+ simulations of the vehicle in an air stream with portable ground and wheels are introduced for various velocities to evaluate the various commitments of pressing factor and shear to lift and haul over the speed range. The back wing offers over 85% of the lift power and 7-8% of the drag power for this specific class of vehicles. At the point when reference is made to the low speed drag and lift coefficients, speeding up from 25 to 100 m/s produces an expansion of Cd of over 3% and a decrease of Cl of over 2%. The results suggest altering the steady lift coefficients and drag coefficients qualities utilized in lap time reenactment tools introducing the classified qualities to add versus the speed of the vehicle [34].

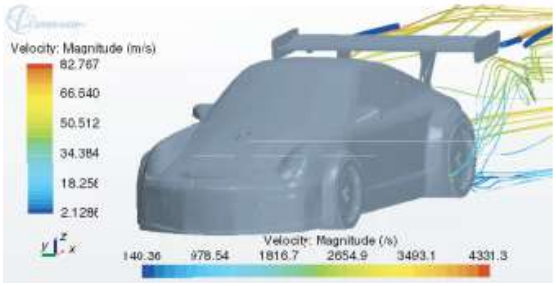

Fig. 19. Vorticity and velocity magnitude at 50 m/s [34]

To research the streamlined conduct of underbody structure in crosswind conditions, two mathematical models were created by applying computational fluid dynamic technique. The anticipated results of feasible k-ε model consistently shows exploratory information, and the relationship deviation of streamlined force is under 10%. By utilizing models of such design, the streamlined force and the air flowing under the vehicle display consistent crosswinds that are mimicked employing underbody structure, and the impact on the streamlined trademark has been examined. It very well may be discovered that the streamlined force expanded essentially under various yaw point. The actual system reaction has been obviously appeared by exploring the airflow around vehicle body by vortices perception method. The consequences of this research can be filled in as a recommendation for examining the model strength of high velocity under crosswind [35].

1.5. Problem statement

This section speaks about the problems three problems that were encountered during the literature survey:

- **Higher drag coefficients**

Drag of a vehicle is largely affected by its frontal area. To reduce the drag, aerodynamic features such as a spoiler, a diffuser, a splitter can be introduced which will reduce the amount of drag experienced by the vehicle. The spoiler which is fitted on the rear of the vehicle will disrupt the flow of air by pushing it over and around the vehicle. The splitter which is fitted on the bottom end of bumper in the front of the vehicle is essential to balance the flow of air in the front of the vehicle reducing drag.

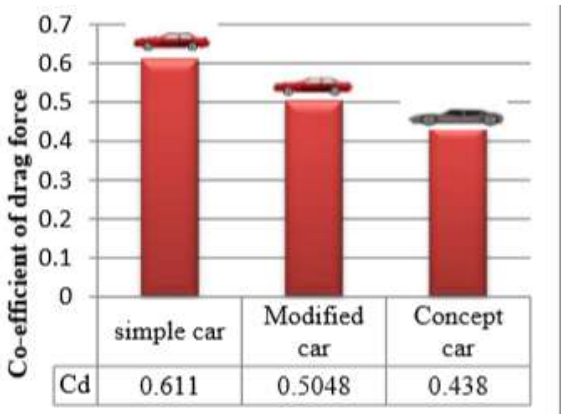

Fig. 20. Drag coefficients of different cars [14]

As the frontal area increases the drag also increases which in turn affects the drag coefficient. When designing the car, the frontal area must be kept in mind. As seen in the Fig. 29 as the frontal area increases the drag coefficient decreases [14].

- **Improper flow separation**

The flow of air around the vehicle starts with laminar flow and gradually transitions to turbulent flow. The flow transition takes place at a point on the roof of the vehicle. Once the flow transitions and becomes turbulent the drag of the vehicle increases. The longer the point of transition is delayed, better the drag that will be obtained. With the addition of a spoiler, a splitter, a diffuser, and a side skirts to the vehicle the flow of air will remain in the laminar state as long as possible. With these devices the drag of the vehicle will considerably reduce as the separation in airflow is delayed hence improving the flow of air around the vehicle and decreasing drag.

- **As downforce increases, drag increases**

This is where the addition of diffuser and optimization of the angle of attack of the spoiler comes into play. At a certain angle of attack of the spoiler the flow of air will be better divided into the lower and upper surface. This reduces the drag which is faced by the spoiler. The diffuser installed

on the lower side of the car will help counteract this effect as it directs the air below the car creating a region of low pressure which increases the downforce on the vehicle. This will in turn will help increase the downforce of the vehicle imparting better stability and traction [15].

The above statements are the general problems faced by a car and with the detailed study from literature review we aim to enhance the aerodynamic performance of a car by the addition of aerodynamic parts such as a spoiler, a splitter, a diffuser, and a side skirt. Once the parts are designed, we then analyze them at different speeds, angles, and heights as per our requirement. Compare the results of the stock car with the modified version of it and choose the best settings for the car with least drag and lift coefficients.

2. Methodology of project

This chapter contains the procedure and detailed explanation of the model, aerodynamic features and the analysis performed using the SolidWorks software. The experiment is conducted by initially running a complete analysis on the stock car. The result of drag coefficient and lift coefficient acquired after the analysis are compared with the results of the car with aerodynamic features.

2.1. Concept and software

The general method to find the aerodynamic parameters of a car is by using a wind tunnel. Experiments using wind tunnels have been performed on cars, but this method is time consuming and at the same time highly expensive. This drawback of the wind tunnel led to the invention of a simulative method to study the aerodynamic parameters numerically. This method was called Computational Fluid Dynamics (CFD) [19]. Computational Fluid Dynamics is used for simulating the design for aerodynamics. It gives the desired numerical solution to the equations in the region of the flow. CFD can solve larger problems hence proving to be an excellent tool.

CFD is a piece of fluid mechanics that uses numerical assessment and data information to separate and handle issues that incorporate progression of fluids. Software is used to calculate the assessments expected to replicate the free stream of the liquid, and the relationship of the fluids that is gases and liquids with surfaces portrayed by limit conditions. With quick supercomputers, better courses of action can be refined, and are routinely expected to address the greatest and most complex issues. Consistent investigation yields programs that improves the speed and precision of complex circumstances. Beginning endorsement of such projects are typically performed using preliminary mechanical assemblies. In addition, as of late performed shrewd or experimental assessment of a particular issue can be used for correlation. A last validation is regularly performed using full-scale testing.

For the investigation of the model designed a detailed CFD study is undertaken in Solidworks with the help of flow simulation. The flow simulation approach in Solidworks depends on two primary standards the first one being, Direct utilization of local CAD as the wellspring of calculation data and secondly, the combination of full 3D CFD demonstrating with less difficult designing techniques in the cases where the cross-section goal is inadequate for full 3D reenactment.

The Solidworks Flow Simulation development relies upon the usage of Cartesian-based mesh and its innovation is one of the basic segments of the CAD/CFD associate for CAD-introduced CFD. The focal points of Cartesian lattice are its effortlessness, speed, and energy of the cross-section computation especially while dealing with local CAD data, minimization of local truncation errors and lastly its power of the differential arrangement.

Solidworks Flow Simulation can think about both laminar and turbulent streams. Laminar streams happen at low estimations of the Reynolds number, which is characterized as the result of sizes of speed and length isolated by the kinematic thickness. At the point when the Reynolds number

surpasses a specific basic value the stream changes easily to violent. To anticipate tempestuous streams, the Favre-found the middle value of Navier-Stokes conditions are utilized, where time-arrived at the midpoint of impacts of the stream disturbance on the stream boundaries are thought of, while the enormous scope, time-subordinates are considered straightforwardly.

Through this strategy, additional terms known as the Reynolds stresses show up in the conditions for which extra data should be given. To close this arrangement of conditions, Solidworks Flow Recreation utilizes transport conditions for the tempestuous active energy and its dissemination rate, utilizing the k-ε model. In liquid regions Solidworks Flow Simulation solves the Navier-Stokes conditions, which are formulas of mass, energy conservation and force laws [37]:

$$\frac{\partial \rho}{\partial t} + \frac{\partial (\rho u_i)}{\partial x_i} = 0; \tag{2.1}$$

$$\frac{\partial (\rho u_i)}{\partial t} + \frac{\partial (\rho u_i u_j)}{\partial x_j} + \frac{\partial P}{\partial x_i} = \frac{\partial \left(\tau_{ij} \tau_{ij}^R\right)}{\partial x_j} + S_i; \tag{2.2}$$

$$\frac{\partial \rho H}{\partial t} + \frac{\partial (\rho u_i H)}{\partial x_i} = \frac{\partial}{\partial x_i}\left(u_j\left(\tau_{ij} + \tau_{ij}^R\right) + q_i\right) + \frac{\partial P}{\partial t} - \tau_{ij}^R \frac{\partial u_i}{\partial x_j} + \rho\varepsilon + S_i + Q_H; \tag{2.3}$$

$$H = h + \frac{u^2}{2}; \tag{2.4}$$

where:

t – time;

ρ – Density;

τ – stress;

q – Heat Flow;

P – pressure.

There are three phases in CFD:

1. Preprocessing
- Using computer aided design, the geometry and physical boundaries are defined. The data input is then processed, and the extraction of volume takes place.
- The volume is then divided into small mesh. The mesh created may be structured or unstructured, consisting of polyhedral, pyramidal, prismatic, tetrahedral, hexahedral elements.
- The model is then defined.
- The definition of boundary conditions is specified.

2. Simulation starts and iteratively the equations are executed in a steady or transition state.

3. In the final stage analysis of the results along with visualization is done using a postprocessor [20].

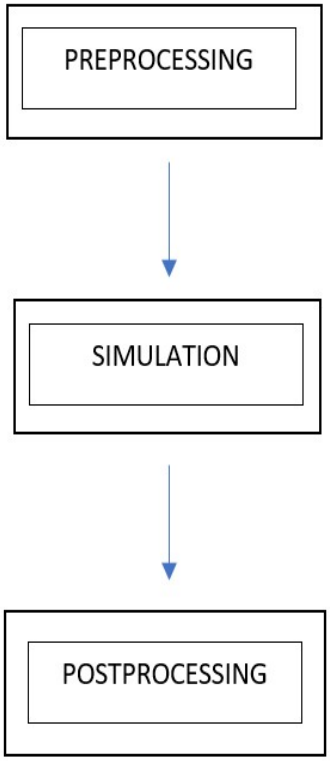

Fig. 21. Three stages of CFD

2.2. Configuration setup

In this experiment there are four aerodynamic parts which are added to the stock car, a diffuser, a splitter, a side skirts and a spoiler. The four features are mated to the stock car and analysis is performed at different configurations, at a standard velocity of 40 m/s. The configurations being:

1. Spoiler
2. Spoiler + Diffuser
3. Spoiler + Side skirts
4. Spoiler + Splitter
5. Spoiler + Diffuser + Side skirts
6. Spoiler + Diffuser + Splitter
7. Spoiler + Diffuser + Splitter + Side skirts

2.3. Modelling of the car

Selection of the model is an important factor in the analytical study of lift and drag coefficients. In this study the car chosen for investigation is a Sports Utility Vehicle (SUV) Mazda CX-9 2020. The model is designed in SolidWorks as a surface model and then converted as a solid model.

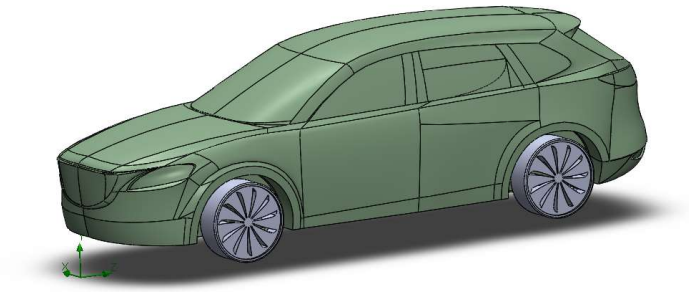

Fig. 22. Model of the stock car Mazda CX-9

Table 1. Dimensions of the stock car as per design

No.	Dimensions	Unit (mm)
1.	Length	5075
2.	Width	1830
3.	Height	1717
4.	Wheelbase	2941
5.	Ground Clearance	205

The model shown in the Fig.22 is designed approximately to real world dimensions using SolidWorks. The focus of this study is to reduce the lift and drag coefficients of the stock car by addition of aerodynamic features such as a spoiler, a diffuser, a splitter, and a side skirts to improve the handling condition, stability and traction of the vehicle.

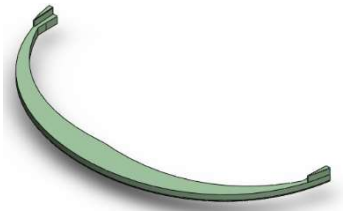

Fig. 23. Splitter

Table 2. Dimensions of splitter

No.	Dimensions	Unit (mm)
1.	Length	1747
2.	Arc Length	2420
3.	Height	20

In the above Fig.23 is the splitter, this is attached to the bottom of the front bumper of the car. As the name suggests, it acts like a wedge splitting the air flowing in front of the car. The high-pressure air flows over the car pushing it down hence resulting in increased traction and downforce as the low-pressure air flows below.

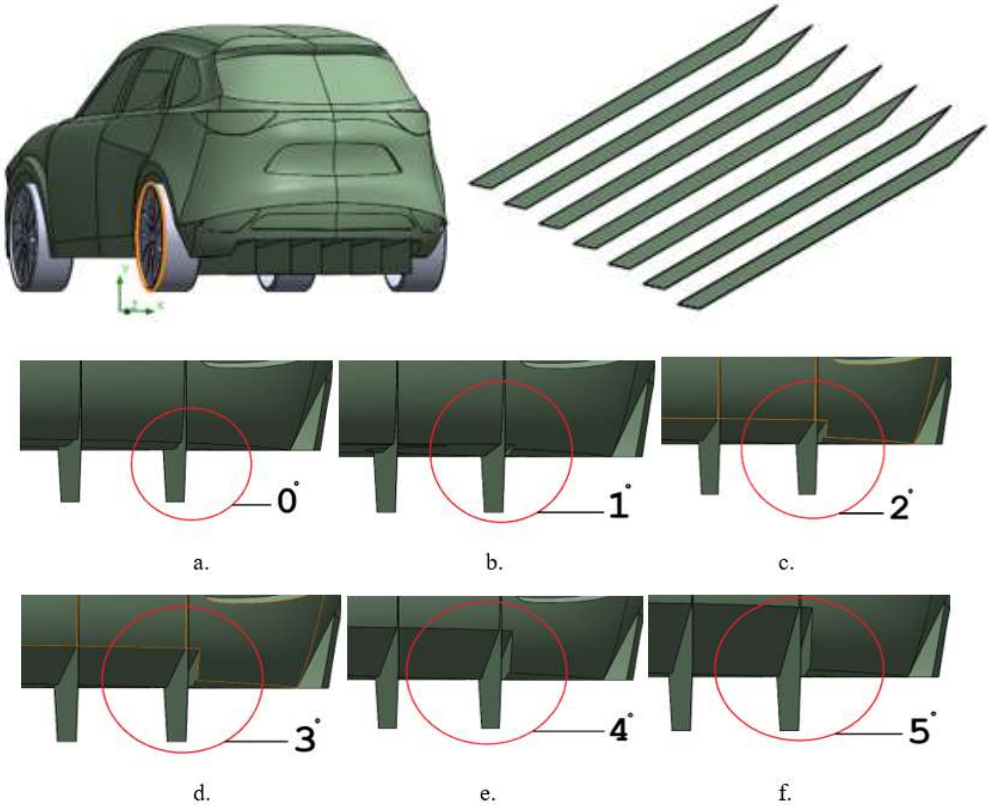

Fig. 24. Diffuser with angles of inclinations as indicated (a) - 0˚ angle, (b) - 1˚ angle, (c) - 2˚ angle, (d) - 3˚ angle, (e) - 4˚ angle, (f) - 5˚ angle

Table 3. Diffuser dimensions as per design

No.	Dimensions	Unit (mm)
1.	Length	1700
2.	Width	1
3.	Height	230

The design in Fig.24 is the diffuser, a section shaped at the rear end of the car. It helps improve the airflow underneath the car giving it a smooth transition of air by reducing the turbulence. From the Fig. 24 (a, b, c, d, e, f), six angles of inclination for the diffuser that in 0˚, 1˚, 2˚, 3˚, 4˚, 5˚ as follows, is designed, and tested at four different speeds at different intervals. Analysis is performed for conditions mentioned above and from the results, the angle with the least drag and lift

coefficient is determined. The key aspect of the feature is to increase the velocity of airflow underneath the car which simultaneously increase the downforce of the car by creating a region of low pressure which leads to suction of the car to the road surface.

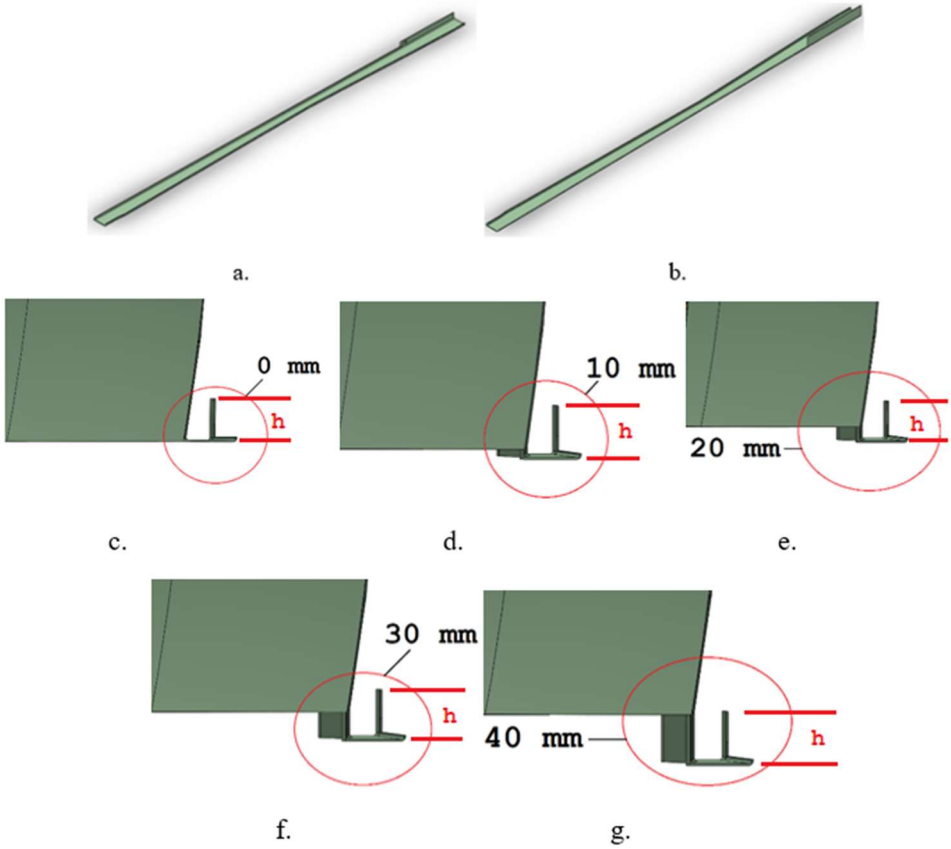

Fig. 25. (a) - Right side skirt, (b) - Left side skirt, (c) – side skirt at 0 mm from ground surface, (d) - side skirt at 10 mm from ground surface, (e) - side skirt at 20 mm from ground surface, (f) - side skirt at 30 mm from ground surface, (g) - side skirt at 40 mm from ground surface

Table 4. Dimensions of side skirts

No.	Dimensions	Unit (mm)
1.	Length	1507
2.	Width	62
3.	Height	2

In Fig.25 the side skirt is a feature meant to reduce the high-pressure air flow on the sides of the car to transcend under it, thus increasing downforce. The closer the car is to the ground, the more efficient it gets. From the Fig. 25 (c, d, e, f, g), five different heights of the side skirt with respect to the ground surface at 205 mm, 215 mm, 225 mm, 235 mm, 245 mm respectively, is designed and tested at four different speeds at different intervals. Analysis is performed for conditions

mentioned above and from the results, the angle with the least drag and lift coefficient is determined.

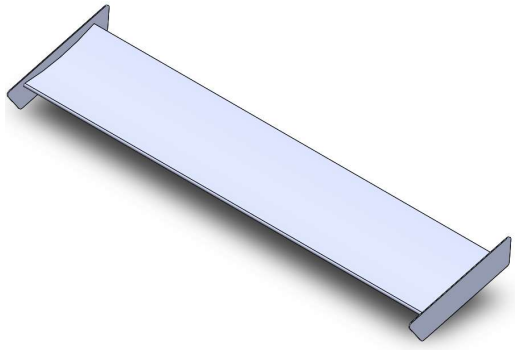

Fig. 26. Spoiler

Table 5. Spoiler dimensions as per design

No.	Dimensions		Unit (mm)
1.	Length		1405, 250
2.	Wing - Diameter		R10
3.	Wing - Arc Angles	Upper	R609
		Lower	R 552
4.	Height		78

Fig.26 shown above is the spoiler, as the name suggests it spoils the air flow on the rear end of the car disrupting and preventing lift and simultaneously decreases the turbulent air flowing at the rear of the car which in turn reduces the drag experienced by the vehicle.

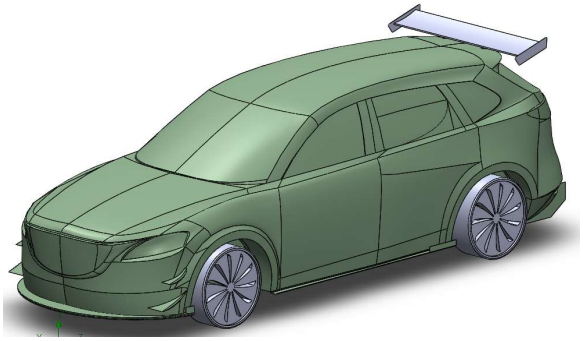

Fig. 27. Stock car with all the aerodynamic feature added

Fig.27 expresses all the aerodynamic features, the splitter, the diffuser, the side skirt, the spoiler attached to the car. At first the stock car as shown in Fig. 22 is analyzed. Once it is completed, the car along with the aerodynamic parts are tested at different configuration as mentioned undergoing analysis at four different speeds, the results attained are set as base results.

2.4. Boundary conditions

The boundary conditions are set to the model to constraint the input variables for the simulation as per our requirements for the experiment. The input speed for the stock car and the car configurations are set as mentioned in the Table.2. The conditions for the road surface are set as real wall, giving it a velocity as same as that of the input velocity of the stock car and configurations as mentioned below.

Table 6. Boundary conditions

Boundary	Boundary Condition	Value
Inlet – Stock car	Velocity	U_z = 20 m/s, 30 m/s, 40 m/s, 50 m/s
Inlet – Configurations	Constant velocity	U_z = 40 m/s
Floor – Stock car	Moving wall	U_z = 20 m/s, 30 m/s, 40 m/s, 50 m/s
Floor – Configurations	Moving wall	U_z = 40 m/s
Car	No slip wall	-
Other walls	Free slip wall	-
Fluid properties	Type	Air
	Density	1.22 kg/m^3
	Pressure	101325 Pa
	Temperature	293.2 K

2.5. Computational domain setup

To perform a CFD analysis a new project is created for flow simulation in SolidWorks. A computational domain is setup in such a way that there are 3 car length distance in front and 5 car length distance behind the model designed. Road surface is mated tangent to the wheels of the car and the computational domain is restricted to the road surface along the X–axis and Z-axis. The different input velocities given are also input to the road surface, ensuring that the road surface also travels at the same velocity as the input velocity.

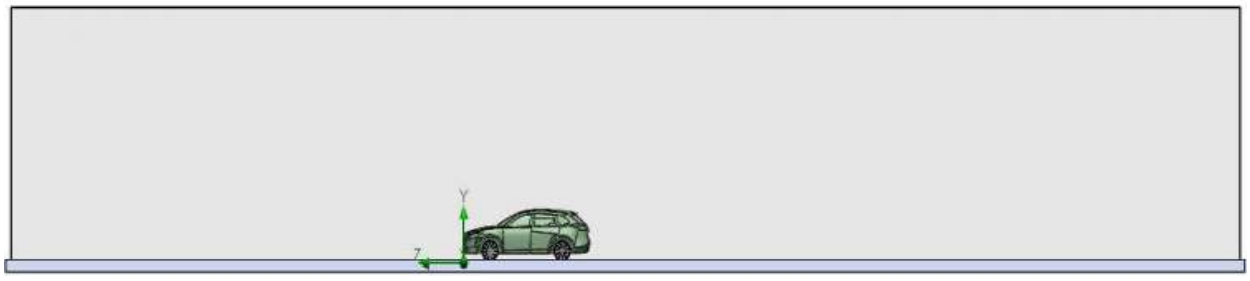

Fig. 28. Computational Domain

Table 7. Dimensions of the computational domain defined for analysis

Axis	Distance (mm)
+X	4400
-X	-4400
+Y	5000
-Y	0
+Z	15000
-Z	-25000

2.6. Meshing

The mesh of the car model is shown in Fig.29. The mesh for the whole computational domain is setup at level 4 which is a moderate mesh and an equidistant refined local mesh at two layers for the car is setup at level 5 giving it a tight uniform mesh as well as defining a multilayer transition with cell refinement of 0.001 m and 0.0011 m.

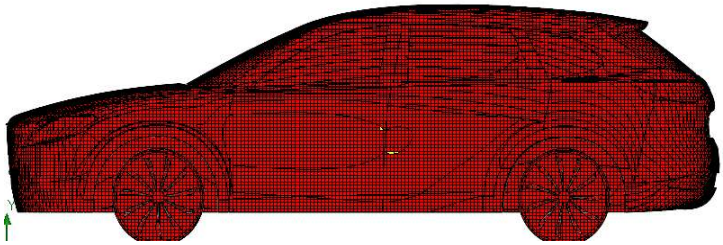

Fig. 29. Mesh of the stock car

3. Result and Discussion

3.1. CFD analysis of the stock car

Once the computational domain is setup, analysis for the stock car is performed. As the analysis is performed at four different speeds the inlet velocity is varied at four different speeds. This enables us to compare the results of the stock car with results of the car setup at different configurations. Once the analysis is completed a pressure cut plot and velocity cut plot for all the speeds are plotted.

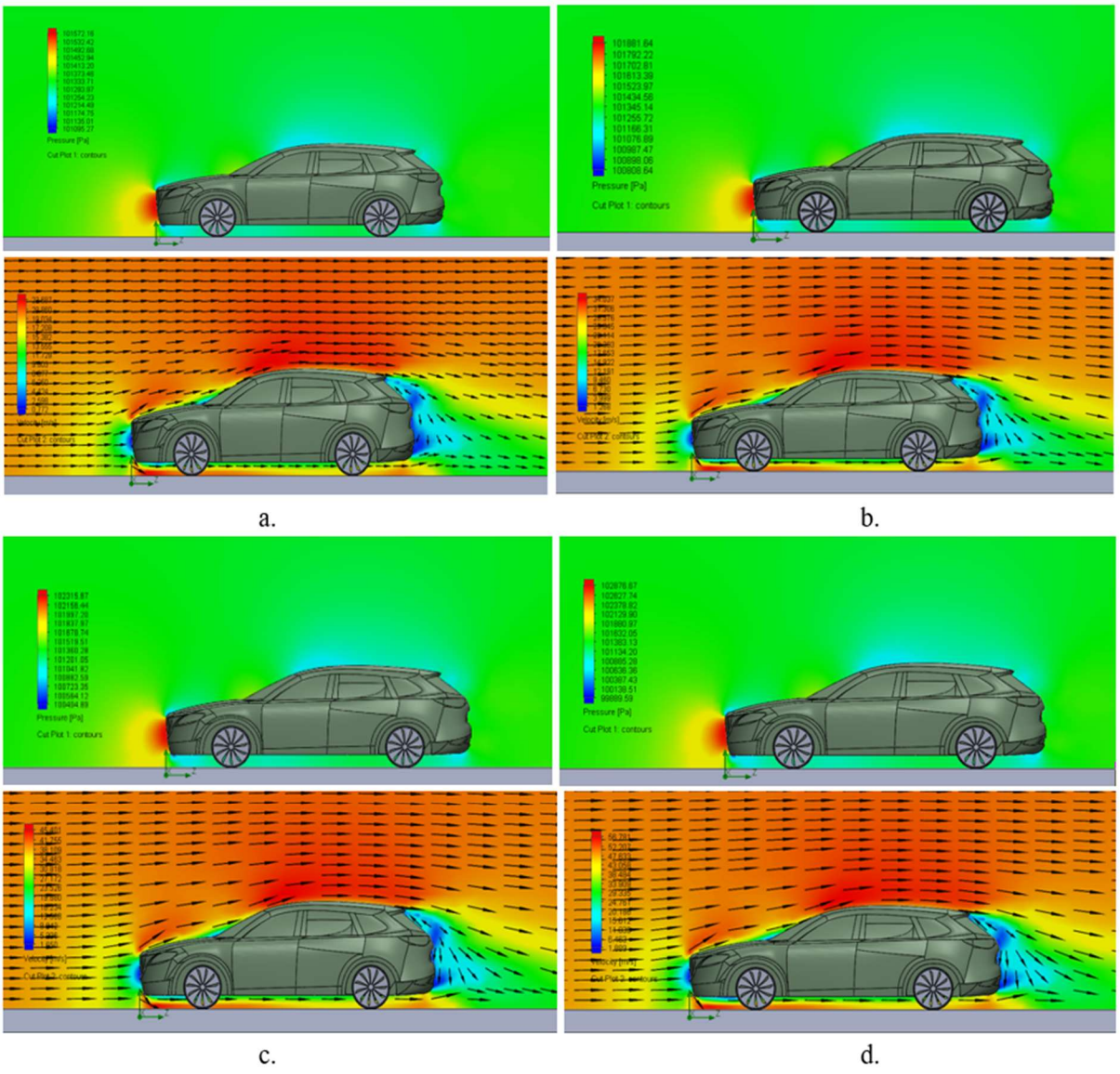

Fig. 30. Velocity and pressure cut plots obtained for the stock car after analysis is performed for different velocities: (a) - velocity and pressure plot at 20 m/s, (b) - velocity and pressure plot at 30 m/s, (c) - velocity and pressure plot at 40 m/s, (d) - velocity and pressure plot at 50 m/s

From the above figure we can see that in the pressure cut plot, high pressure is generated at the front end of the car and the pressure gradually decreases as the air flows over the car and there are a few areas of high pressure created on the lower and upper surface of the car. From the velocity cut plot the flow of air over the car is laminar and then turns turbulent at the rear end once it passes over the car.

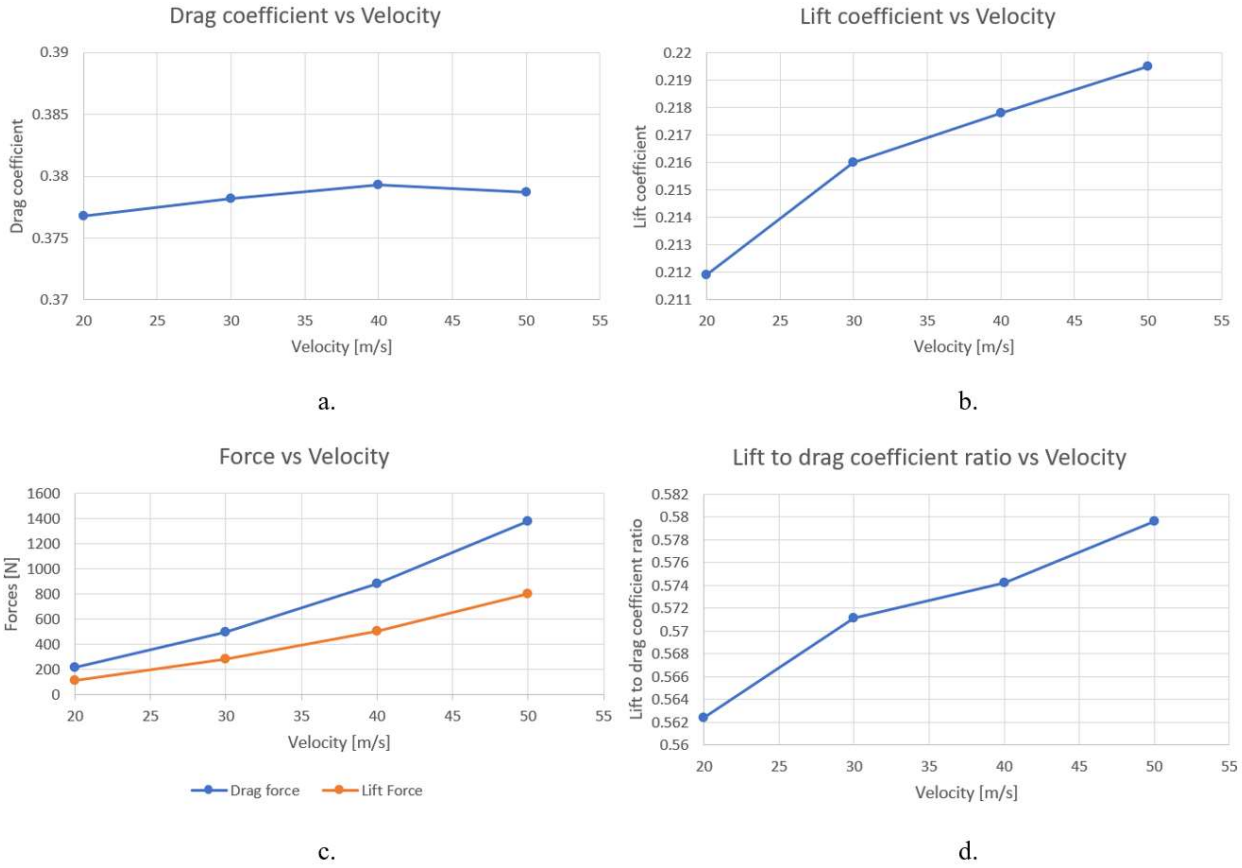

Fig. 31. Results obtained after the analysis of the stock car, with (a) - Drag coefficient vs Velocity, (b) - Lift coefficient vs Velocity, (c) - Force vs Velocity, (d) - Lift to Drag coefficient ratio vs Velocity

From the graph (a) it is noticed that with the increase in velocity the drag increases from 20 m/s to 40 m/s and decreases at 50 m/s. With respect to the lift coefficient versus the velocity indicated in graph (b) there is a steady increase in lift coefficient as the velocity increases. In the graph (d), the curve has a steady increase in the lift to drag coefficient since the values of both the drag coefficient and the lift coefficient increases. Graph (c), shows a gradual increase in the drag force increasing from a minimum value of 214N up to a maximum of 1375N. Likewise, the lift force increases from a minimum value of 113N to a maximum value of 800N.

3.2. CFD analysis of the diffuser

Analysis for the stock car with the diffuser at four different speeds is carried out. The model is executed for the speeds mentioned and at 6 different angles 0˚, 1˚, 2˚, 3˚, 4˚, 5˚ as described in

Fig.24. Tests are performed at different angles of diffuser inclination with respect to speed. The results obtained from the analysis is represented in the form of a graph. This is performed to identify the appropriate angle with least lift and drag coefficients.

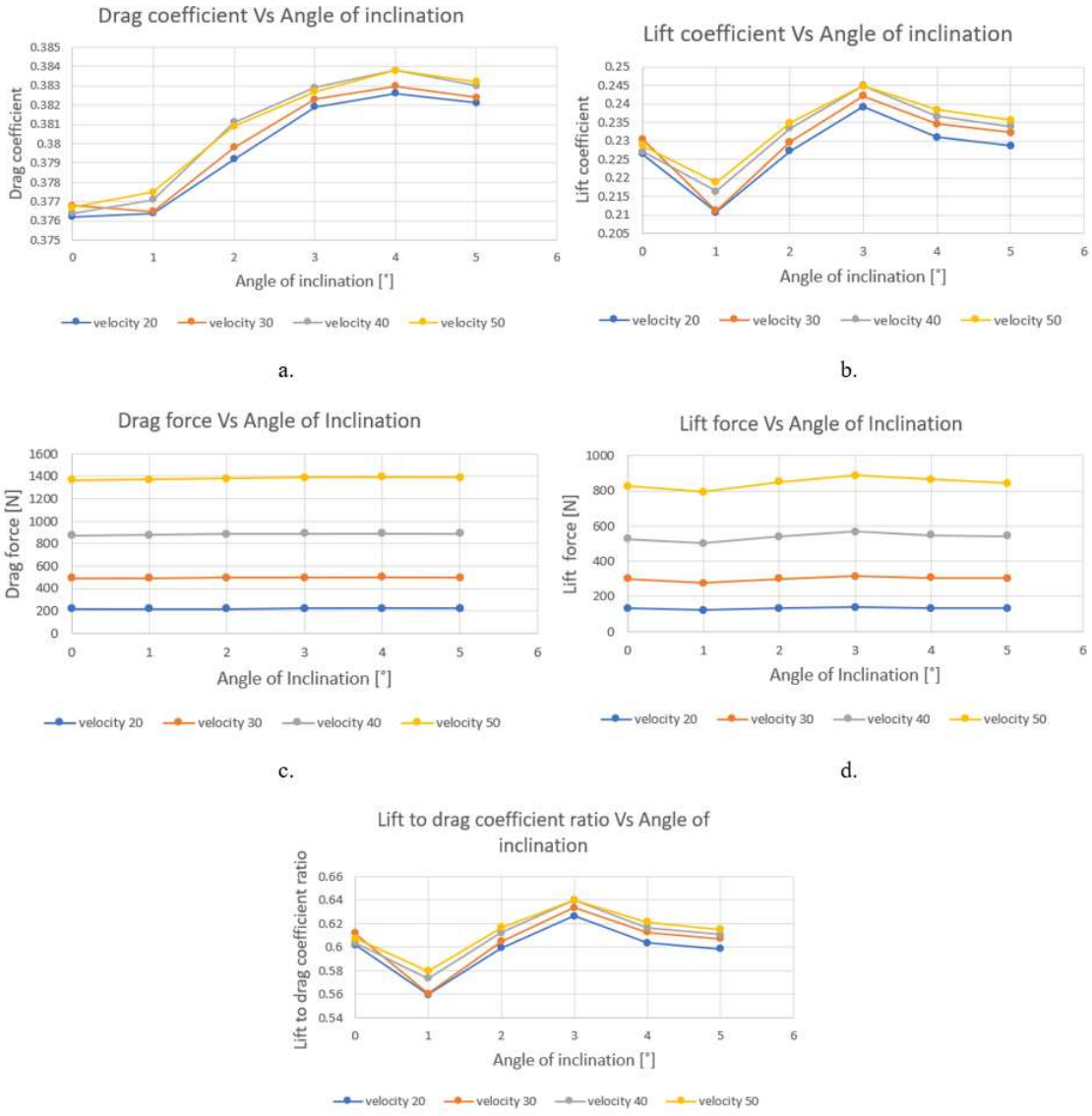

Fig. 32. Result of the diffuser with stock car for different angles of inclination with respect to different speeds, (a) - Drag coefficient vs Inclination angle, (b) - Lift coefficient vs Inclination angle, (c) - Drag force vs Inclination angle, (d) - Lift force vs Inclination angle, (e) – Lift to Drag coefficient vs Inclination angle

Graph (c) and (d) representing the drag and lift forces notifies a steady increase with increase in Inclination angle with respect to speed. Graph (a) displays decrease in drag coefficients at angle 1˚ and gradually increases with increase in diffuser inclination angle. The lift coefficient in graph

(b) indicates similar result as that of graph (a). From the results obtained we observe that angle 1˚ has the least drag and lift coefficients in comparison to other angles. This angle 1˚ is considered as the standard angle of setup for the diffuser in the configuration setup.

3.3. CFD analysis of the side skirt

Analysis for the stock car with the side skirt at four different speeds is run. Tests are performed at heights of 205 mm, 215 mm, 225 mm, 235 mm, and 245 mm with respect to the ground. The results obtained from the analysis is tabulated in the form of a graph. This is performed to identify the appropriate height of the side skirt with least lift and drag coefficients with respect to the road surface.

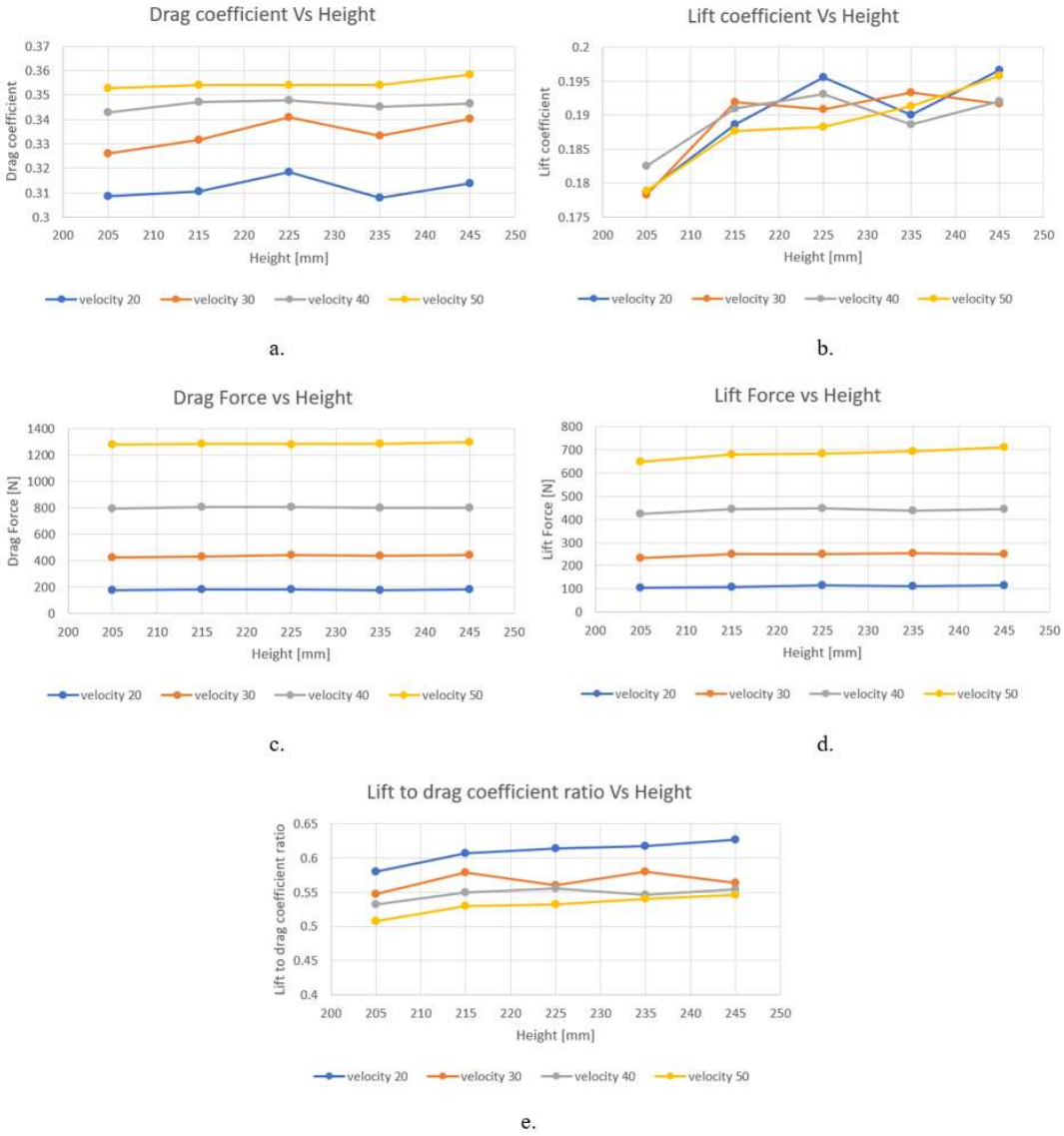

Fig. 33. Result of the side skirt with stock car for different heights with respect to road surface (a) - Drag coefficient vs Inclination angle, (b) - Lift coefficient vs Inclination angle, (c) - Drag force vs Inclination angle, (d) - Lift force vs Inclination angle, (e) – Lift to Drag coefficient vs Inclination angle

Graph (c) and (d) representing the drag and lift forces notifies a steady increase with increase height of the side skirt with respect to the road surface. At low speeds in graph (a), drag coefficient is observed to increase and decrease with change in height, whereas at higher speeds the drag gradually increases. Likewise, the lift coefficient in graph (b) shows similar result as that of graph (a). From the results obtained it is observed that at the height 205 mm which is the stock ground clearance, least drag and lift coefficients are attained. This height of 205 mm is considered as the standard height of the side skirt in the configuration setup.

3.4. CFD analysis of the car with configuration 1 – spoiler

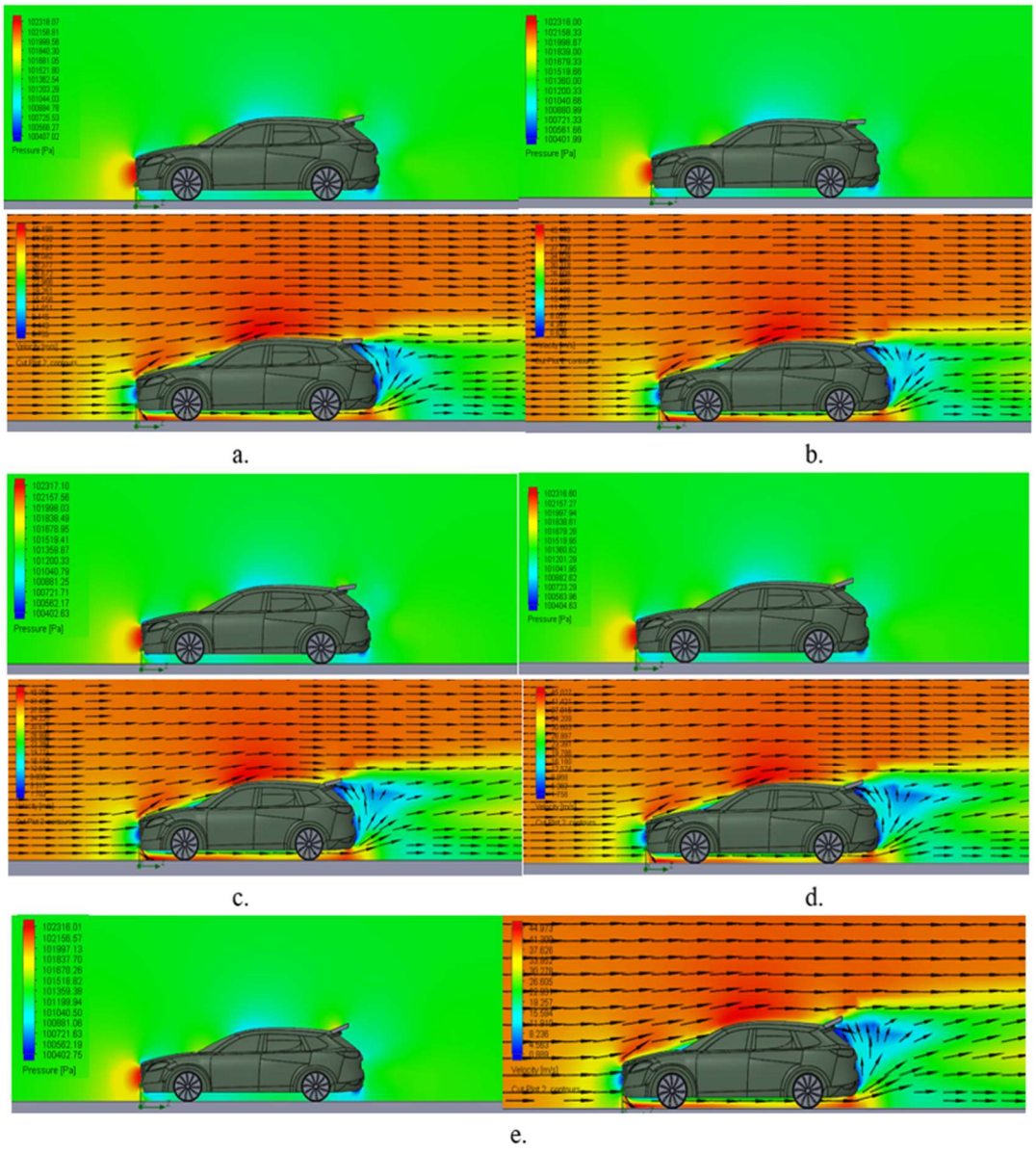

Fig. 34. Velocity and pressure cut plots obtained for the stock car with spoiler after analysis is performed at 40 m/s for different spoiler angles, with (a) - velocity and pressure plot at 0˚, (b) - velocity and pressure plot at 5˚, (c) - velocity and pressure plot at 10˚, (d) velocity and pressure plot at 15˚, (e) velocity and pressure plot at 20˚

Configuration 1 consisting of spoiler is tested at five different angles of inclination 0˚, 5˚, 10˚, 15˚, 20˚. The vehicle has a steep angle downward from the roof to the trunk causing separation in airflow. This causes the airflow to become turbulent creating a region of low pressure. With the addition of spoiler the separation of airflow is delayed creating high pressure region in the front of the spoiler in turn leading to downforce. From the Fig.34, the pressure at the rear upper end of the vehicle near the spoiler increases with increase in inclination angle of the spoiler. Due to this increase in high pressure, lift force decreases and down force gradually increases. Since the spoiler decreases the velocity of air, separation of airflow is delayed further when compared to the stock car inducing downforce. The results obtained are tabulated in the form of graphs in Fig.35. The drag coefficient of the vehicle also increases with increase in spoiler inclination angle.

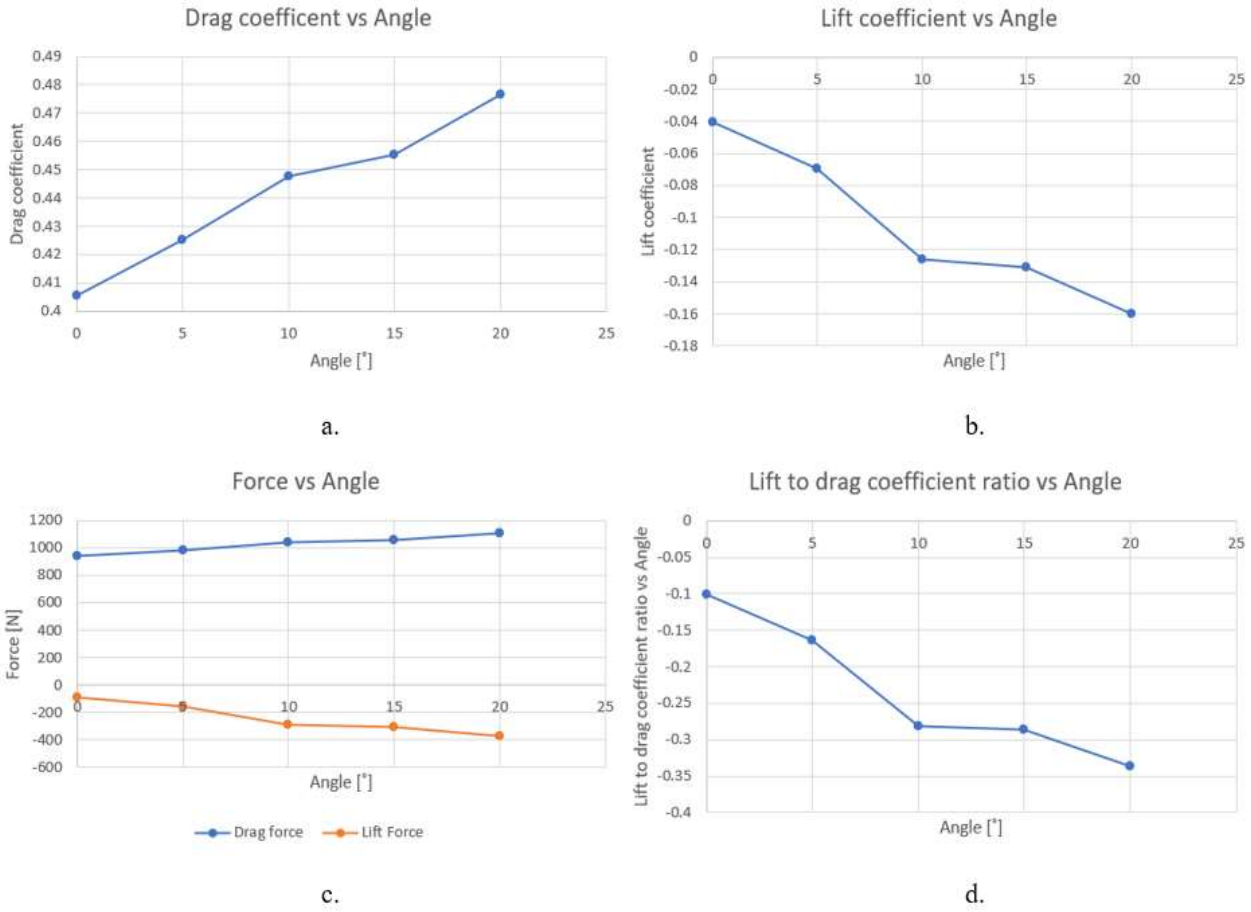

Fig. 35. Results of configuration 1, with (a) - Drag coefficient vs Inclination angle, (b) - Lift coefficient vs Inclination angle, (c) - Forces vs Inclination angle, (d) - Lift to Drag coefficient ratio vs Inclination angle

3.5. CFD analysis of the car with configuration 2 – spoiler + diffuser

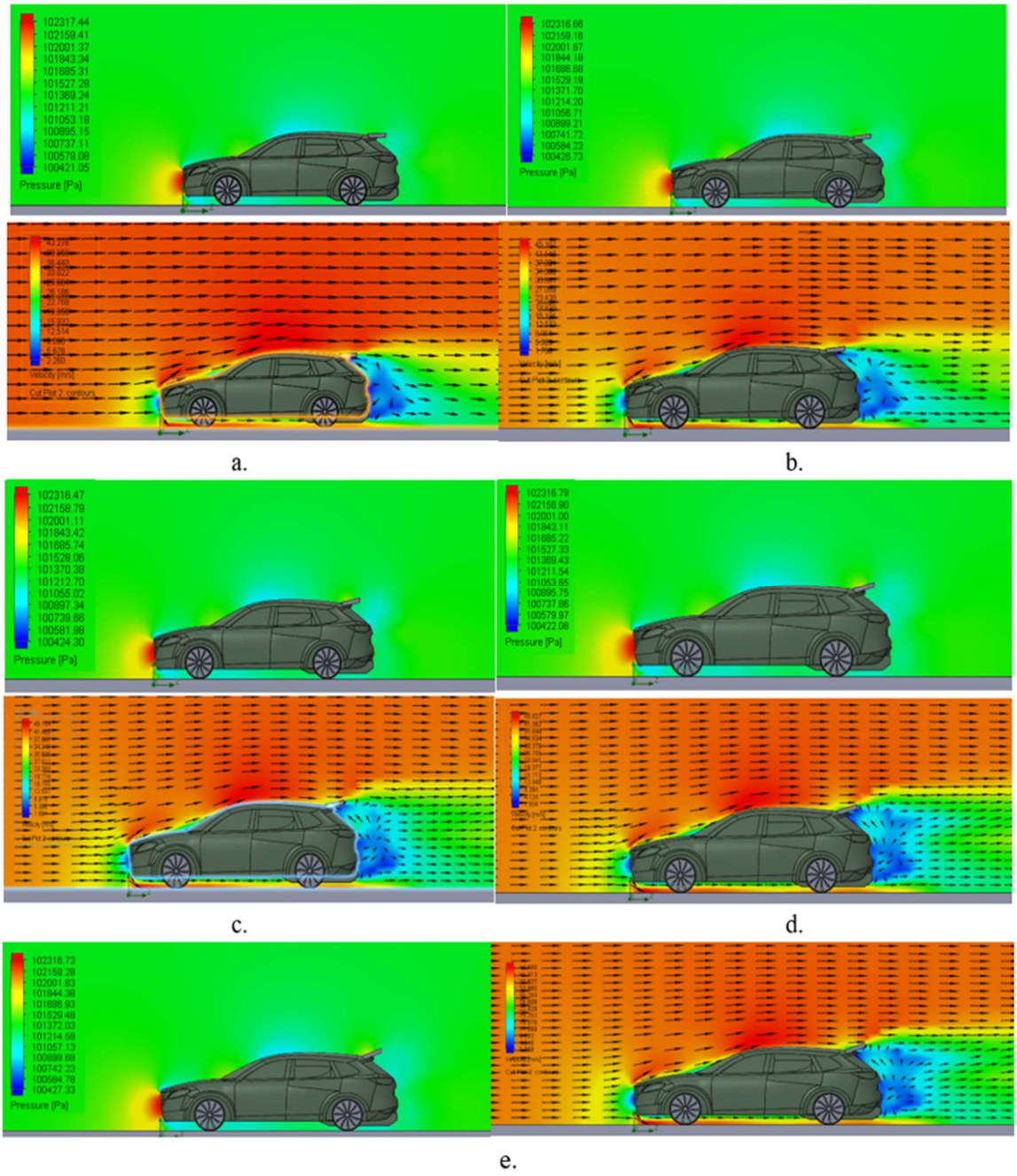

Fig. 36. Velocity and pressure cut plots obtained for the stock car with spoiler and diffuser after analysis is performed at 40 m/s for different spoiler angles: (a) - velocity and pressure plot at 0˚, (b) - velocity and pressure plot at 5˚, (c) - velocity and pressure plot at 10˚, (d) - velocity and pressure plot at 15˚, (e) - velocity and pressure plot at 20˚

Configuration 2 consisting of the spoiler and the diffuser is tested at five different angles of spoiler inclination 0˚, 5˚, 10˚, 15˚, 20˚, with a standard diffuser angle of 1˚. From the Fig.36, with the introduction of diffuser at the rear lower end of the vehicle a region of low pressure is created.

This is because the air flowing under the car generally travels at a lower speed when compared to the air flowing over it. The diffuser behaves as a guide vanes guiding the flow of air. Hence, the low velocity air flowing under the car is converted to high velocity and a region of low pressure. This low pressure under the car creates a suction to the road surface reducing the effect of lift and increasing the downforce.

From the velocity plot in Fig.36 it is indicated that the separation of air flow is further delayed with the addition of diffuser. The pressure at the rear end of the vehicle near the spoiler increases with increase in inclination angle of the spoiler. Due to this increase in high pressure, lift force decreases and down force gradually increases. The results in Fig.37 indicate that the drag coefficient of the vehicle simultaneously increases with increase in spoiler inclination angle and is inverse in case of lift coefficient. The spoiler delays separation of airflow, creating high pressure region in the front of the spoiler in turn leading to downforce.

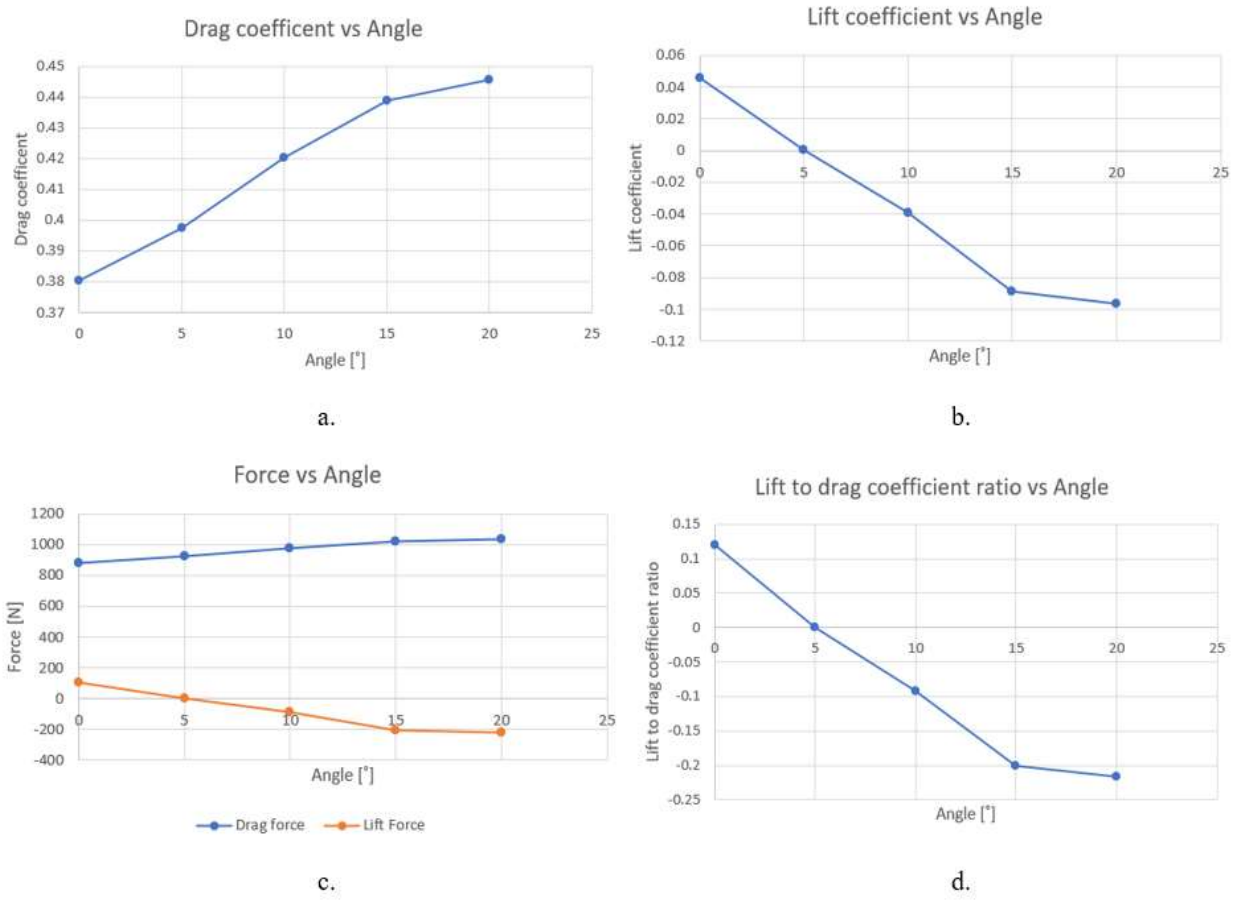

Fig. 37. Results of configuration 2, with (a) - Drag coefficient vs Inclination angle, (b) - Lift coefficient vs Inclination angle, (c) - Forces vs Inclination angle, (d) - Lift to Drag coefficient ratio vs Inclination angle

3.6. CFD analysis of the car with configuration 3 – spoiler + sideskirt

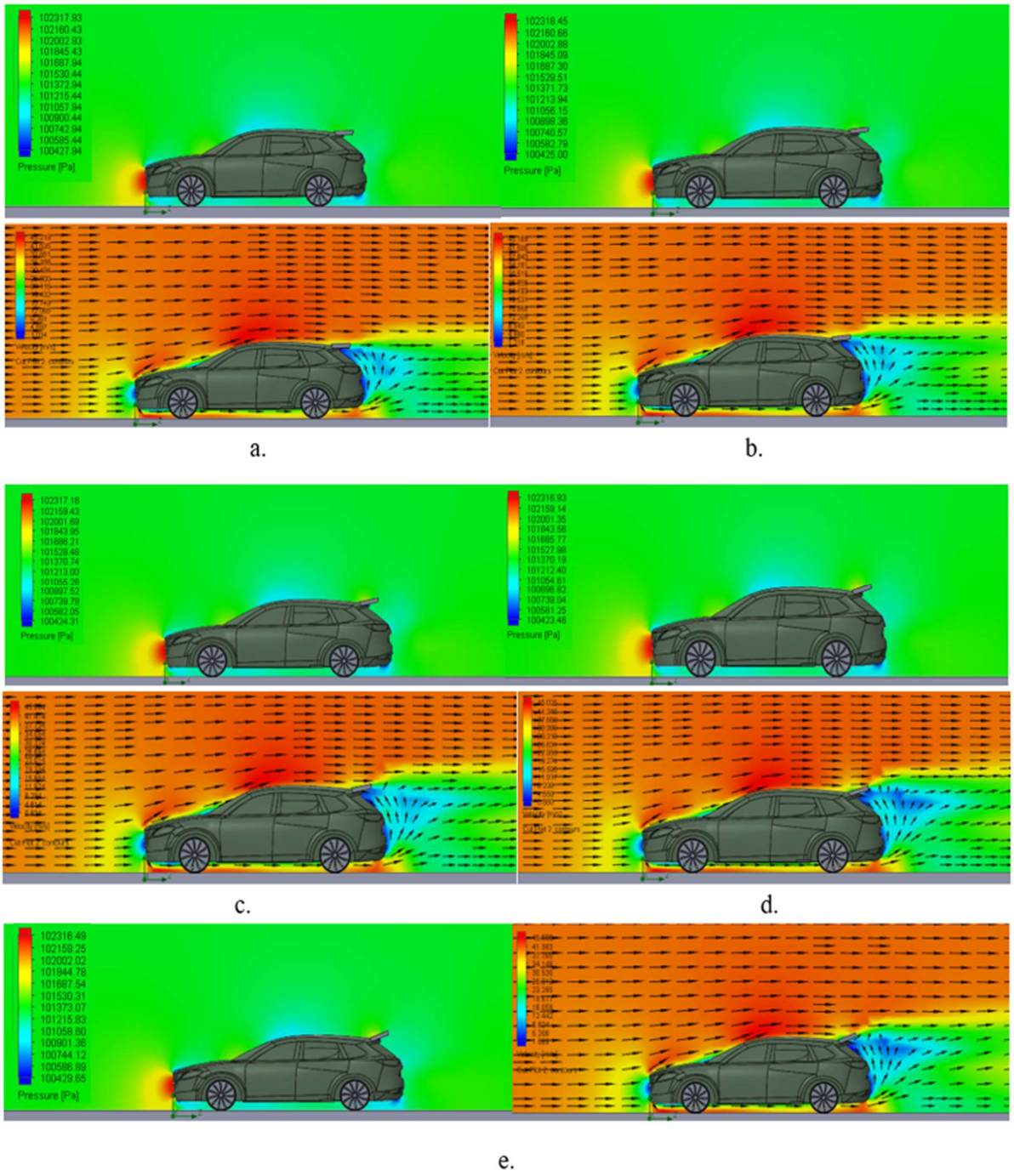

Fig. 38. Velocity and pressure cut plots obtained for the stock car with spoiler and side skirt after analysis is performed at 40 m/s for different spoiler angles: (a) - velocity and pressure plot at 0˚, (b) - velocity and pressure plot at 5˚, (c) - velocity and pressure plot at 10˚, (d) - velocity and pressure plot at 15˚, (e) - velocity and pressure plot at 20˚

Configuration 3 consists of the spoiler and the side skirt is tested at five different angles of spoiler inclination 0˚, 5˚, 10˚, 15˚, 20˚, with a standard side skirt height of 205 mm. From the Fig.38 it is

observed that pressure plot and velocity plot is similar to that of the configuration 1. Due to the reason being, sideskirts tend to reduce the high pressure air flowing on the sides of the car to the region of low pressure underneath the car. The most important fact is that sideskirt will not reduce the amount of air pressure that flows on the sides of the car, but they beneficially split the bottom of the car into two parts.

Firstly, the underbody attributes high velocity and low pressure, and second the high pressure region on the side of the car. With the absence of this barricade between the two, air from the sides rushes underneath the car resulting in reduction in downforce.

The effectivness of the side skirt is best shown when the car is close to the ground, implying, closer the side skirt is to the ground, greater the downforce generated. In this case the car's lower surface is not very close to the ground, thus the effectiveness is minimal. The spoiler combined with the sideskirt, increases the pressure at the rear end of the vehicle near the spoiler with increase in inclination angle of the spoiler as shown in Fig.38. Due to this increase in high pressure lift force decreases and down force increases. The flow separation of air is delayed with the help of the spoiler, ensuring smooth flow of air.

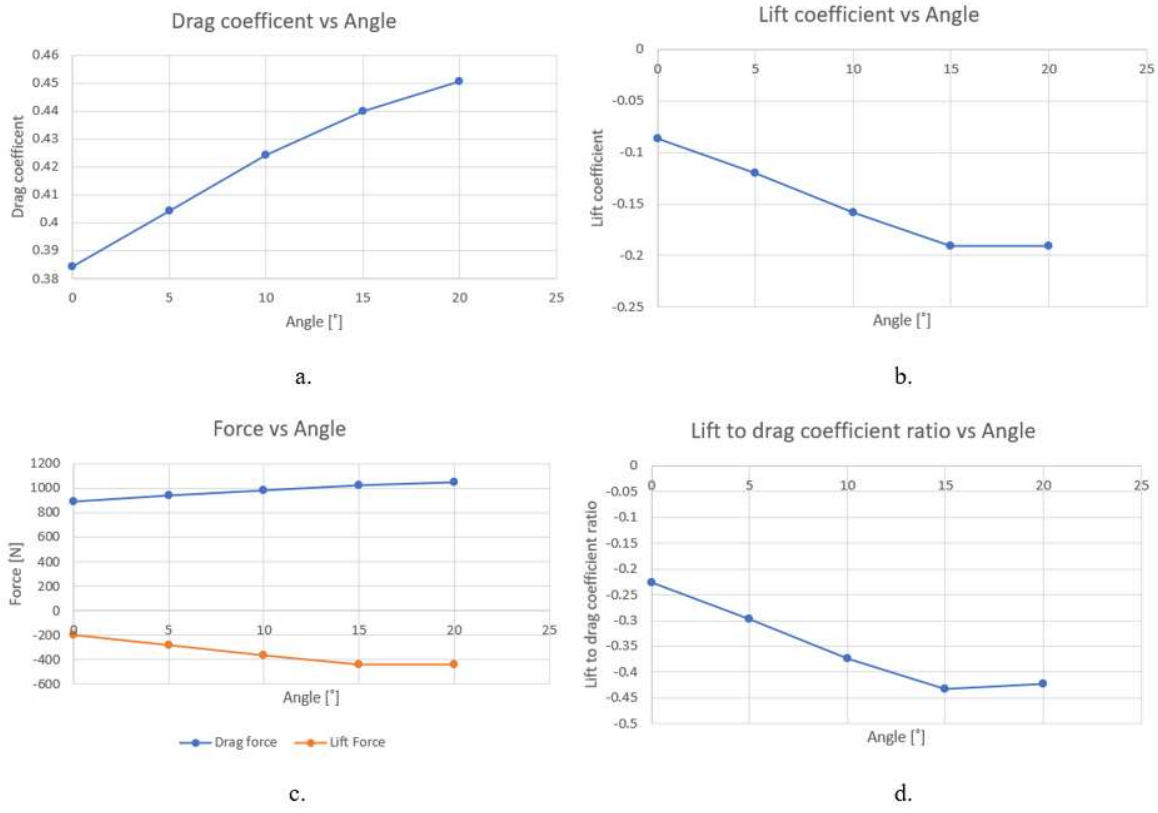

Fig. 39. Results of configuration 3, with (a) - Drag coefficient vs Inclination angle, (b) - Lift coefficient vs Inclination angle, (c) - Forces vs Inclination angle, (d) - Lift to Drag coefficient ratio vs Inclination angle

3.7. CFD analysis of the car with configuration 4 – spoiler + splitter

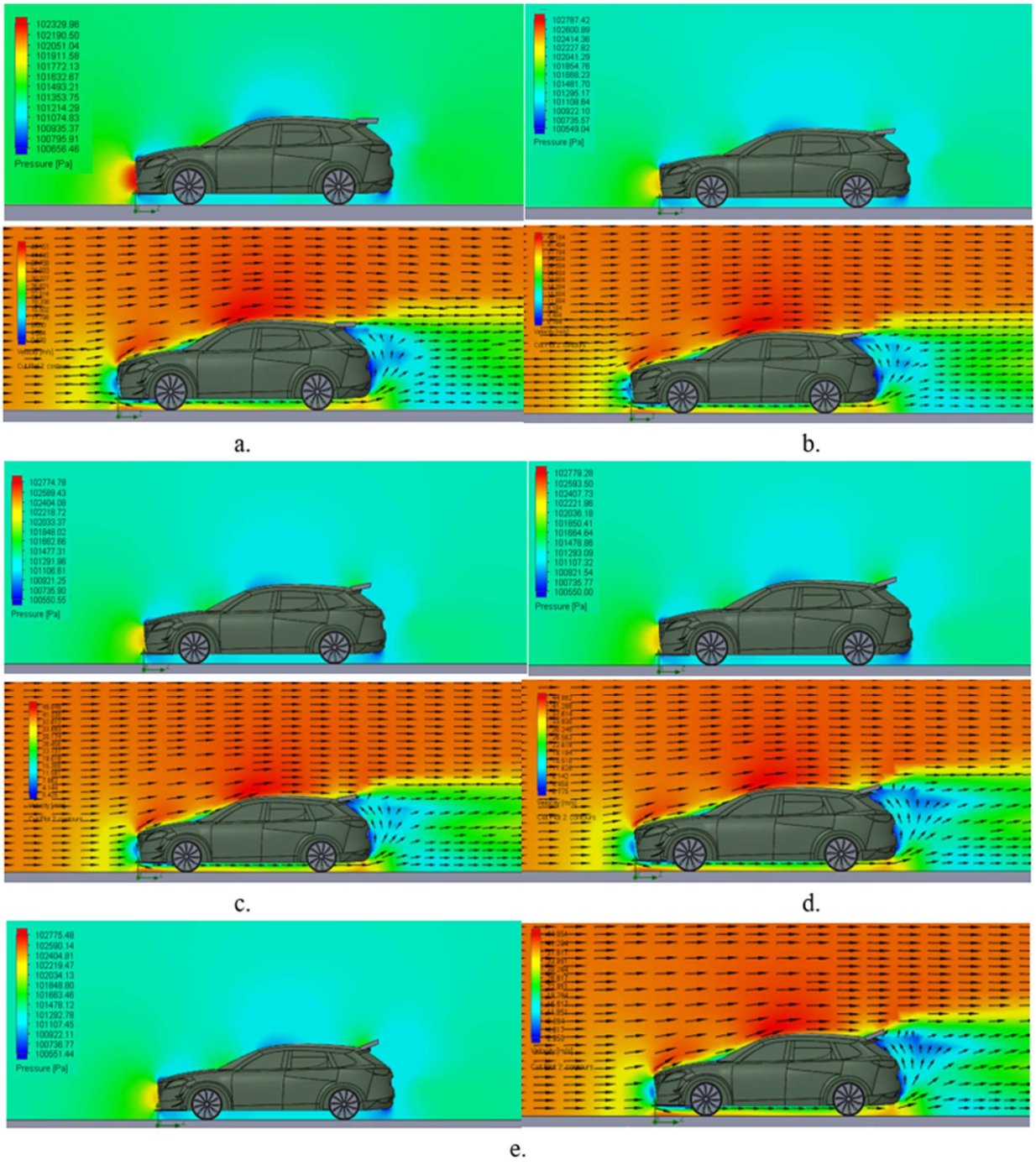

Fig. 40. Velocity and pressure cut plots obtained for the stock car with spoiler and splitter after analysis is performed at 40 m/s for different spoiler angles: (a) - velocity and pressure plot at 0˚, (b) - velocity and pressure plot at 5˚, (c) - velocity and pressure plot at 10˚, (d) - velocity and pressure plot at 15˚, (e) - velocity and pressure plot at 20˚

Configuration 4 consisting of the spoiler and the splitter is tested at five different angles of spoiler inclination 0˚, 5˚, 10˚, 15˚, 20˚. When a vehicle is travelling at greater speeds, at the front end of

the car air pressure is densely built up. Majority of the low velocity high pressure air flows underneath the car. Since high pressure air flows underneath the car, low pressure air tends to flow over the car. Due to this difference in low pressure and high pressure acting on the lower and upper end of the car, the car experiences lift resulting in reduced traction.

From the Fig.40, it is observed that high pressure which was built up around the front bumper of the car starts to flow upwards over the car because of the splitter. Since high pressure air flows over the car, high velocity low pressure air flows underneath the car. This results in increase in downforce helping the car hug the ground providing better traction and stability control. In addition there are two small canards attached to the front of the car these maintain the high pressure air around the car from flowing to the low pressure region underneath the car ensuring better downforce. The spoiler in this case behaves similar to configuration 1, but combined with the splitter the pressure at the rear end of the vehicle increases with increase in inclination angle of the spoiler as seen in graph (a) of Fig.41. Due to this increase in high pressure, lift force decreases as observed in graph (c) and down force increases. The drag coefficient of the vehicle slightly increases with increase in spoiler inclination angle.

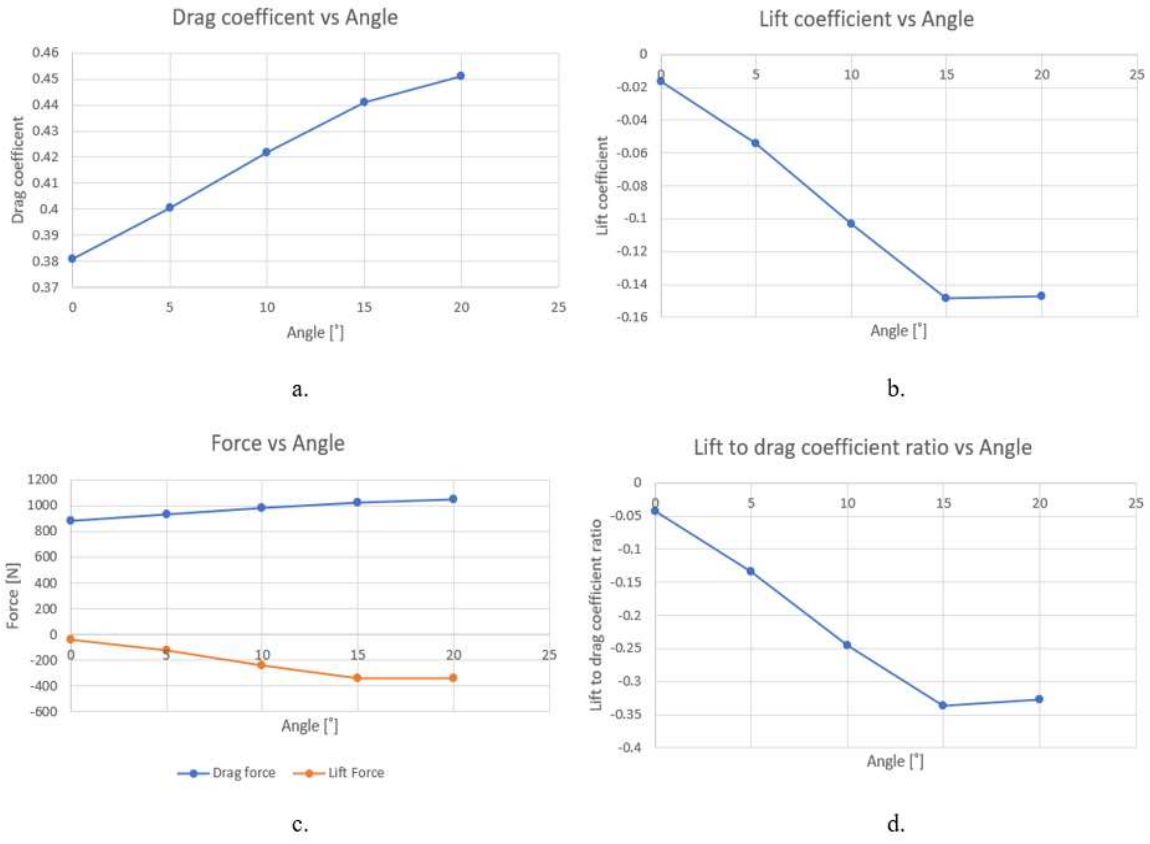

Fig. 41.Results of configuration 4, with (a) - Drag coefficient vs Inclination angle, (b) - Lift coefficient vs Inclination angle, (c) - Forces vs Inclination angle, (d) - Lift to Drag coefficient ratio vs Inclination angle

3.8. CFD analysis of the car with configuration 5 - spoiler + diffuser + side skirt

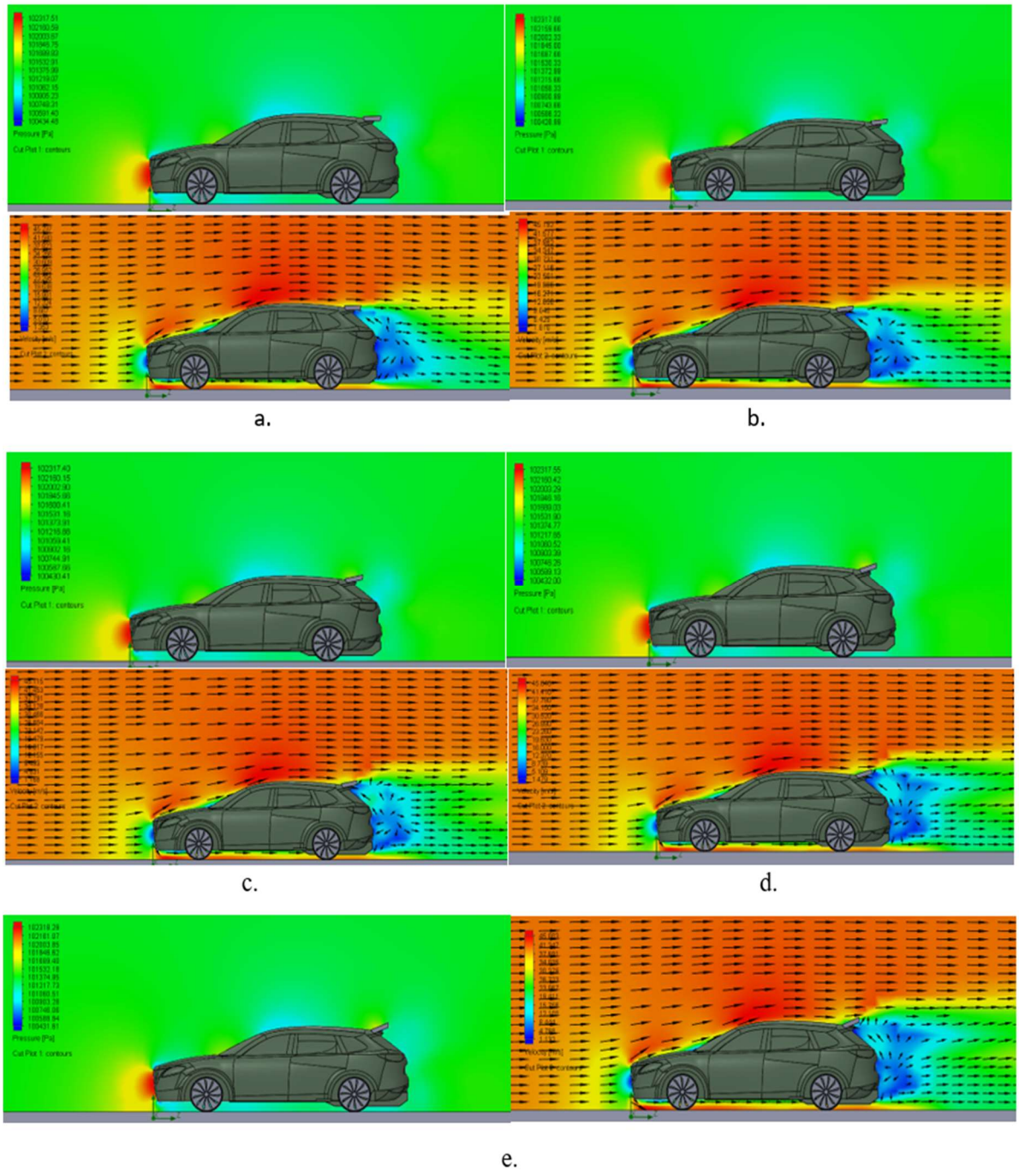

Fig. 42. Velocity and pressure cut plots obtained for the stock car with spoiler, diffuser and side skirt after analysis is performed at 40 m/s for different spoiler angles: (a) - velocity and pressure plot at 0˚, (b) - velocity and pressure plot at 5˚, (c) - velocity and pressure plot at 10˚, (d) - velocity and pressure plot at 15˚, (e) - velocity and pressure plot at 20˚

Configuration 5 consists of a combination of the spoiler, the diffuser and the side skirt is tested at five different angles of spoiler inclination 0˚, 5˚, 10˚, 15˚, 20˚, with a standard diffuser angle of

1˚and side skirt with a height of 205 mm from the road surface. From the Fig.42, with the diffuser at the rear lower end of the vehicle, a region of low pressure is created. This is because the air flowing under the car generally travels at a lower speed when compared to the air flowing over it. The diffuser behaves as a guide vanes guiding the flow of air. This low pressure under the car creates a suction to the road surface reducing the effect of lift and increasing the downforce. The most important fact is that sideskirt will not reduce the amount of air pressure that flows on the sides of the car, but they beneficially split the bottom of the car into two parts.

The effectivness of the side skirt is best shown when it is close to the ground, implying closer the side skirt is to the ground, greater the downforce generated. In this case the sideskirt is not very close to the ground thus the effectiveness is minimal. From the Fig.42, the pressure at the rear end of the vehicle near the spoiler increases with increase in inclination angle of the spoiler, due to this increase in high pressure lift force indicated in Fig.43 (c) decreases and down force gradually increases. From the velocity plot in Fig.42 (a,b,c,d,e) with increase in inclination angle of the spoiler, the separation of air flow is further delayed.

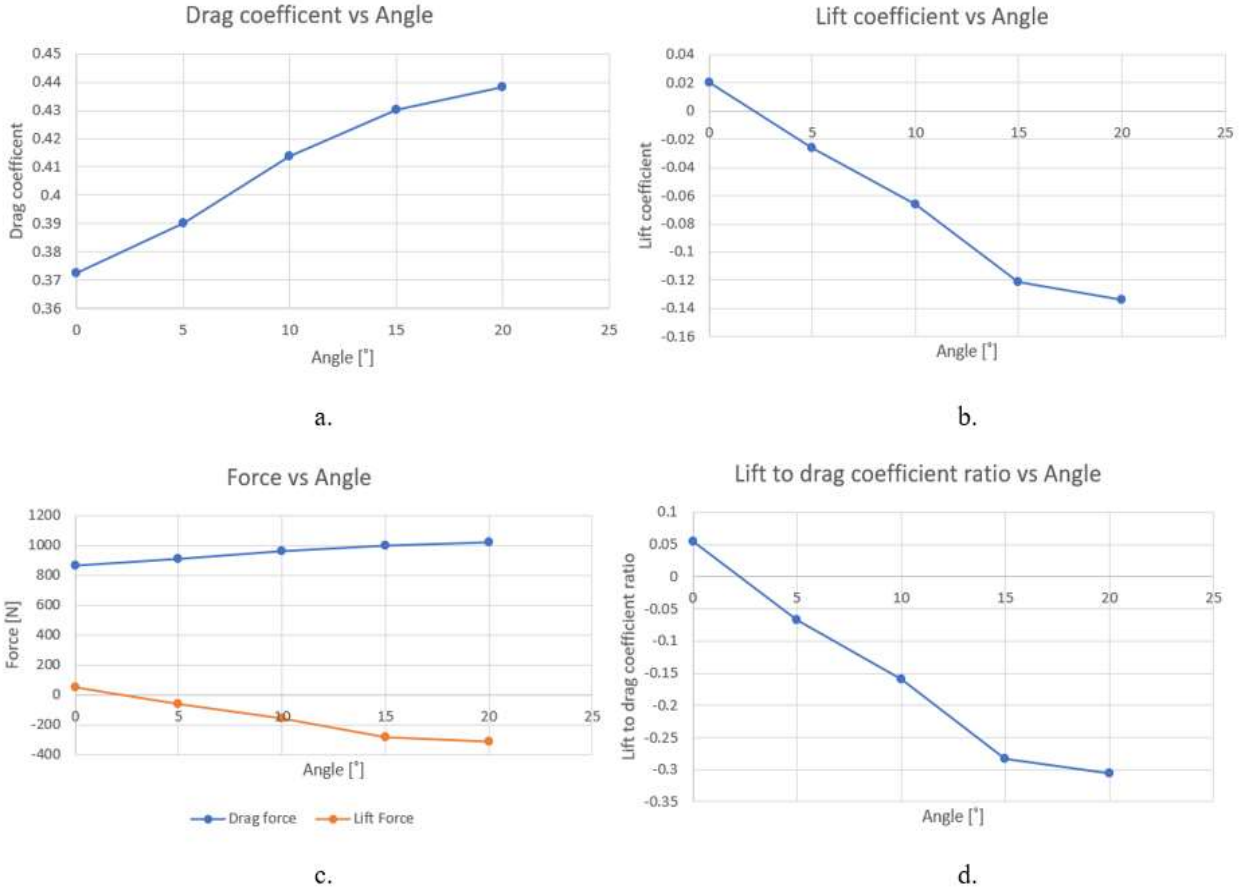

Fig. 43. Results of configuration 5, with (a) - Drag coefficient vs Inclination angle, (b) - Lift coefficient vs Inclination angle, (c) - Forces vs Inclination angle, (d) - Lift to Drag coefficient ratio vs Inclination angle

3.9. CFD analysis of the car with configuration 6 - spoiler + diffuser + splitter

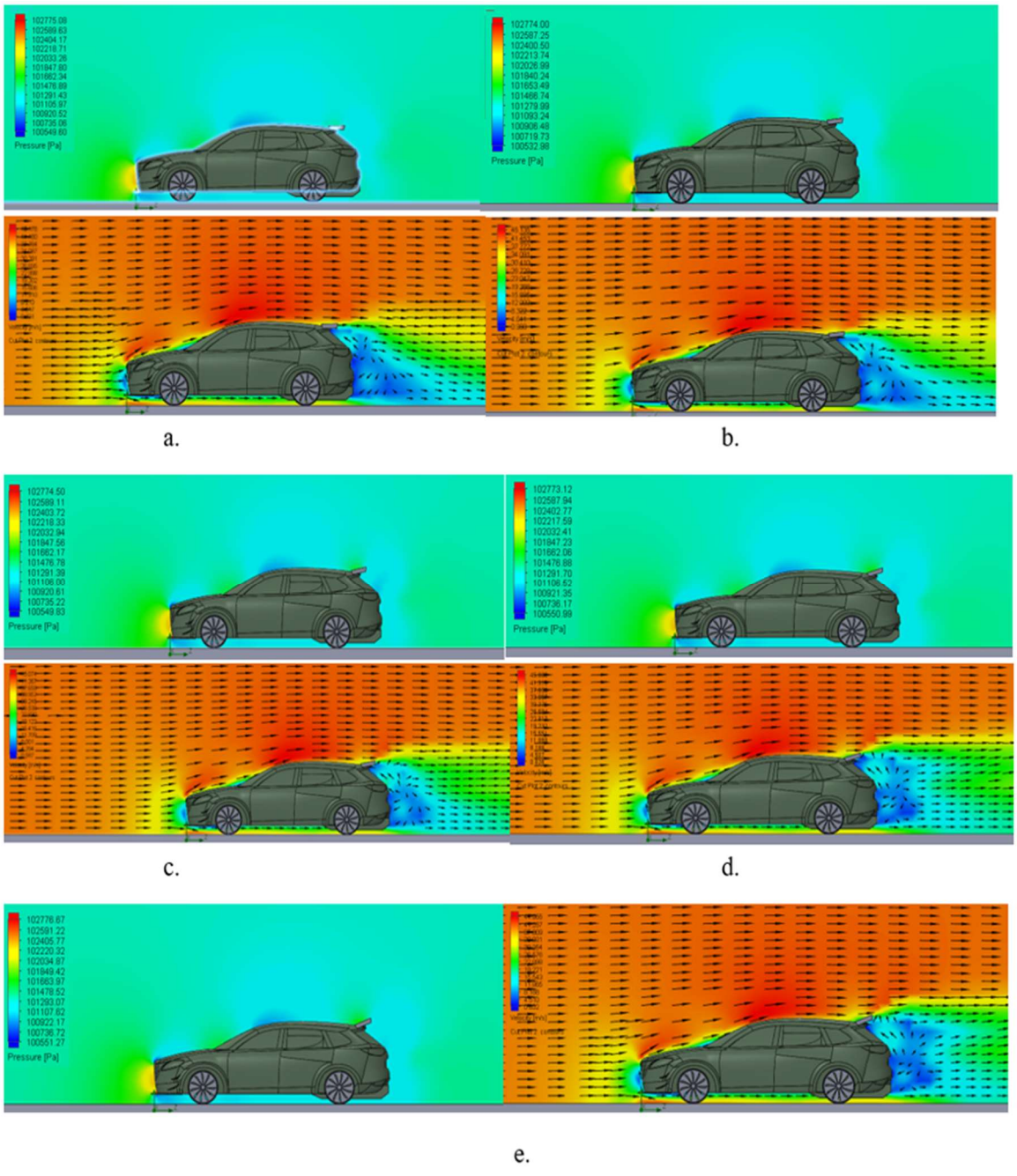

Fig. 44. Velocity and pressure cut plots obtained for the stock car with spoiler, diffuser and splitter after analysis is performed at 40 m/s for different spoiler angles: (a) - velocity and pressure plot at 0˚, (b) - velocity and pressure plot at 5˚, (c) - velocity and pressure plot at 10˚, (d) - velocity and pressure plot at 15˚, (e) - velocity and pressure plot at 20˚

Configuration 6 consists of a combination of the spoiler, the diffuser and the splitter is tested at five different angles of spoiler inclination 0˚, 5˚, 10˚, 15˚, 20˚. From the Fig.44, the pressure at the rear upper end of the vehicle near the spoiler increases with increase in inclination angle of the

spoiler. Due to this increase in high pressure lift force decreases and down force gradually increases.

From the presure plots in Fig.44, at the rear lower end of the vehicle there is decrease in pressure. This is because the air flowing under the car travels at a lower speed when compared to the air flowing over it. The low velocity air flow under the car is converted to high velocity and a region of low pressure. This low pressure under the car creates a suction to the road surface reducing the effect of lift and increasing the downforce. High pressure air flows above the car, low pressure air flows underneath the car. Due to this difference in low pressure and high pressure acting on the lower and upper end of the car, the car experiences lower lift resulting in better traction.

From the figure shown above, it is observed that high pressure which was built up around the front bumper of the car starts to flow upwards over the car because of the splitter. The spoiler combined with the splitter and the diffuser creates a region of high pressure at the rear end of the vehicle near the spoiler which increases with increase in inclination angle of the spoiler. This increase in high pressure causes a decrease in lift force and down force increases. The separation of air flow is delayed in this configuration ensuring a smooth flow of air and reduction in drag. The drag coefficient of the vehicle increases with increase in spoiler inclination angle.

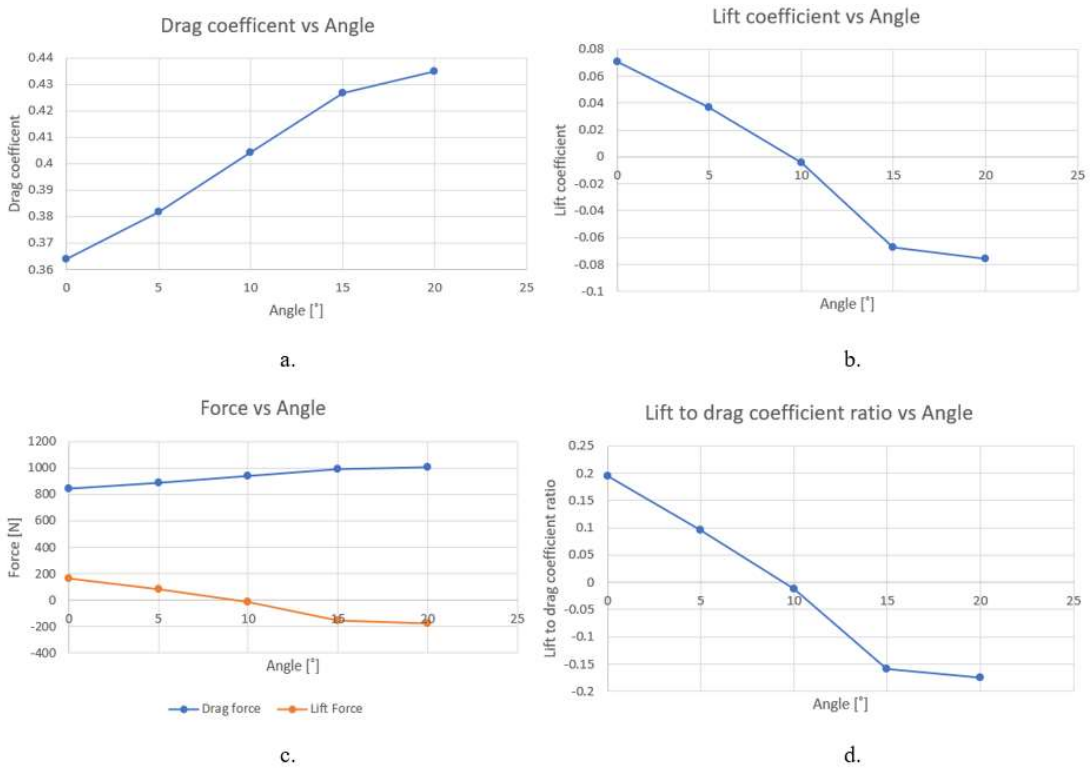

Fig. 45. Results of configuration 6, with (a) - Drag coefficient vs Inclination angle, (b) - Lift coefficient vs Inclination angle, (c) - Forces vs Inclination angle, (d) - Lift to Drag coefficient ratio vs Inclination angle

3.10. CFD analysis of the car with configuration 7 - spoiler + diffuser + splitter + side skirts

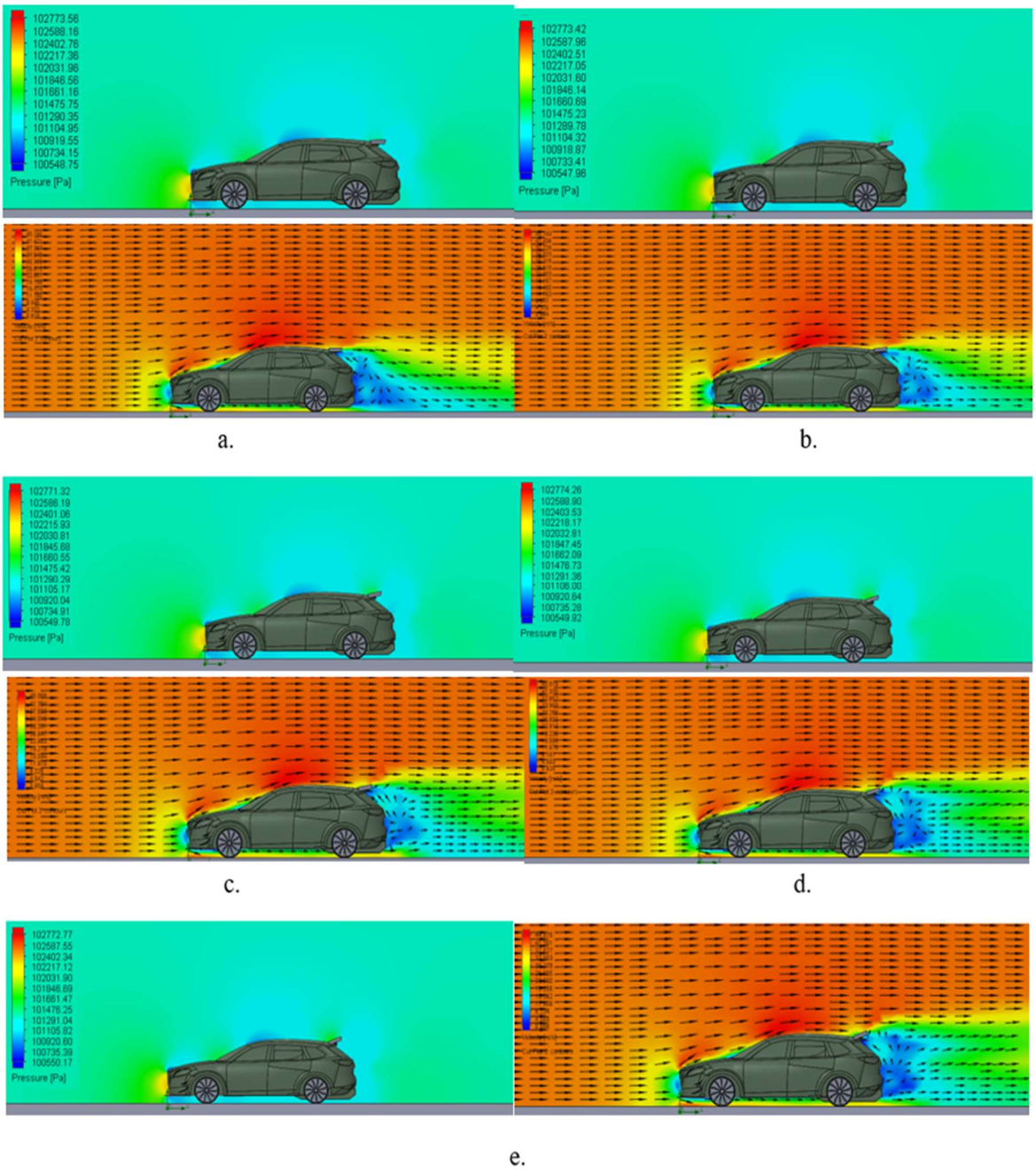

Fig. 46. Velocity and pressure cut plots obtained for the stock car with spoiler, diffuser, side skirt and splitter after analysis is performed at 40 m/s for different spoiler angles: (a) - velocity and pressure plot at 0˚, (b) - velocity and pressure plot at 5˚, (c) - velocity and pressure plot at 10˚, (d) - velocity and pressure plot at 15˚, (e) - velocity and pressure plot at 20˚

Configuration 7 consisting of a combination of all the aerodynamic features the spoiler, the diffuser, the sideskirt and the splitter is tested at five different angles of inclination of spoiler 0˚, 5˚, 10˚, 15˚, 20˚. With the addition of spoiler the separation of airflow is delayed creating high pressure region in the front of the spoiler in turn leading to downforce. From the pressure plot in

Fig.46, the pressure at the rear upper end of the vehicle near the spoiler increases with increase in inclination of the spoiler angle.

With the addition of diffuser at the rear lower end of the vehicle a region of low pressure is created. The air flowing under the car travels at a lower speed when compared to the air flowing over it. This low pressure under the car creates a suction to the road surface reducing the effect of lift and increasing the downforce.

From the Fig.46 shown above, it is observed that high pressure which was built up around the front bumper of the car starts to flow upwards over the car because of the splitter. Since high pressure air flows over the car, high velocity low pressure air flows underneath the car. The effectivness of the side skirt is best shown when it is close to the ground, implying closer the side skirt is to the ground, greater the downforce generated. In this case the sideskirt is not very close to the ground thus the effectiveness is minimal. In the velocity cut plot the spoiler combined with the diffuser, the splitter and the sideskirt causes the better separation of air at the rear end of the vehicle near the spoiler. Fig.47 shows, high pressure lift force decreasing which signifies gradual increase in down force. The flow separation of air is delayed with the help of the aerodynamic features, ensuring smooth flow of air.

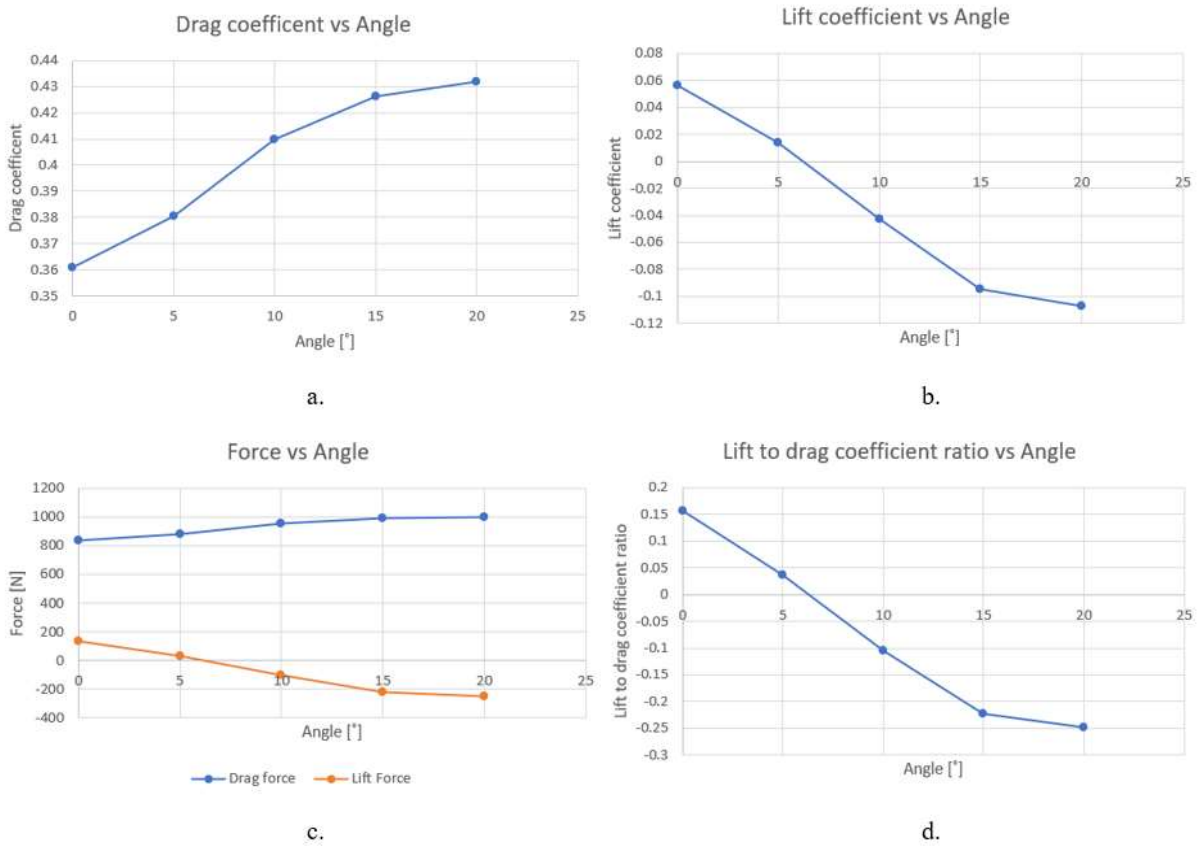

Fig. 47. Results of configuration 7, with (a) - Drag coefficient vs Inclination angle, (b) - Lift coefficient vs Inclination angle, (c) - Forces vs Inclination angle, (d) - Lift to Drag coefficient ratio vs Inclination angle

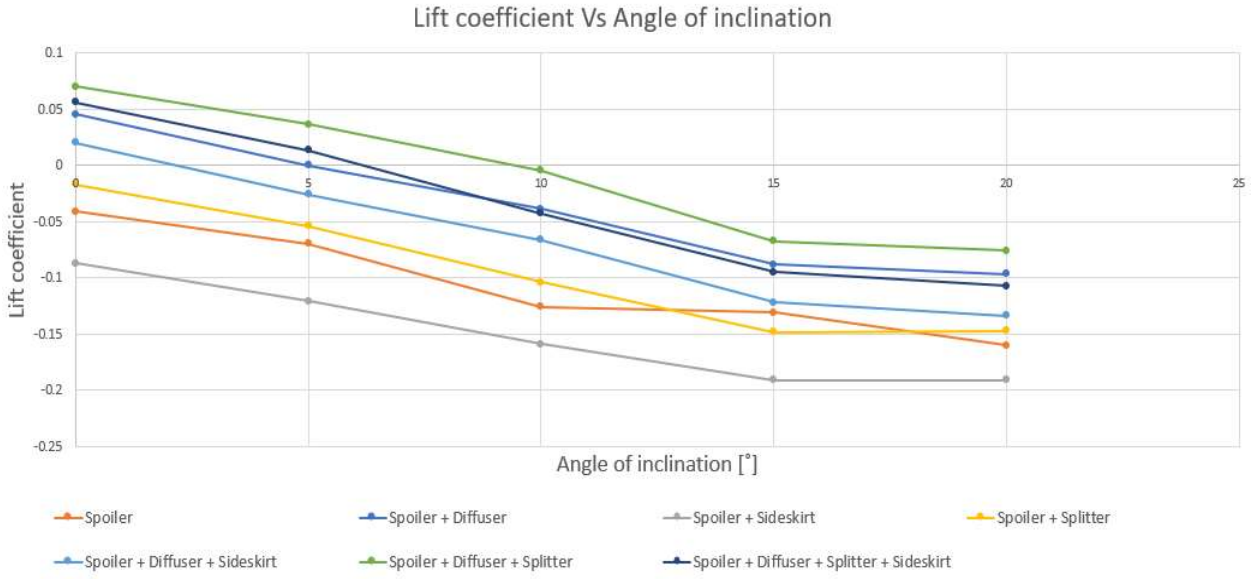

Fig. 48. Lift Coefficient vs Angle of Spoiler Inclination

The graph in Fig.48, displays the seven configurations tested for lift coefficient. The Y-axis represents the lift coefficient Cl and X-axis represents the angle of spoiler inclination. In this case the graph has a steady decrease, the reason being that as the downforce on each tested configuration increases the lift coefficient decreases. This decrease in the lift coefficient is tabulated and a graph has been plotted respectively. Each configuration has different values for the 5 different spoiler inclination angles tested. From the graph it is noted that the spoiler and the side skirt configuration experiences maximum downforce, and the spoiler, the diffuser, and the splitter configuration experience the minimum downforce.

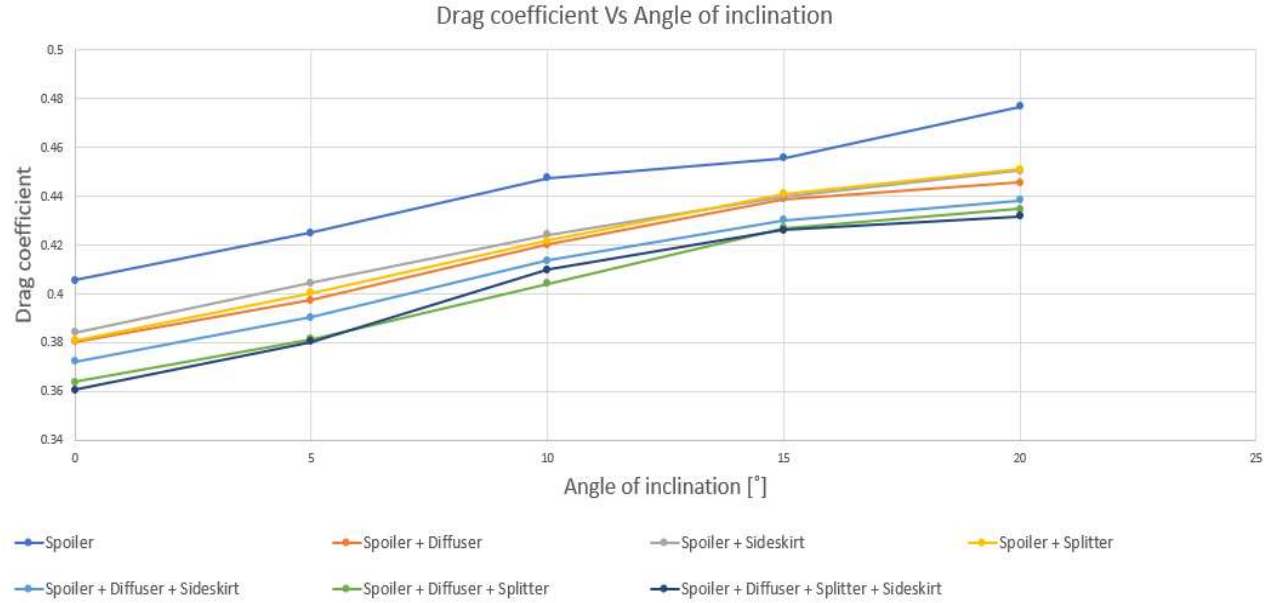

Fig. 49. Drag Coefficient vs Angle of Spoiler Inclination

The graph in Fig.49, presents the seven configurations tested for drag coefficient. The Y-axis represents the drag coefficient Cd and X-axis represents the angle of spoiler inclination. In this case the graph has a steady increase in the drag coefficients. This increase in the drag coefficient is tabulated and a graph has been plotted respectively. Each configuration has different values at the 5 different spoiler inclination angles tested. From the graph it is observed that the spoiler configuration experiences maximum drag, and the configuration with the spoiler, the diffuser, the side skirt, and the splitter experience the least drag.

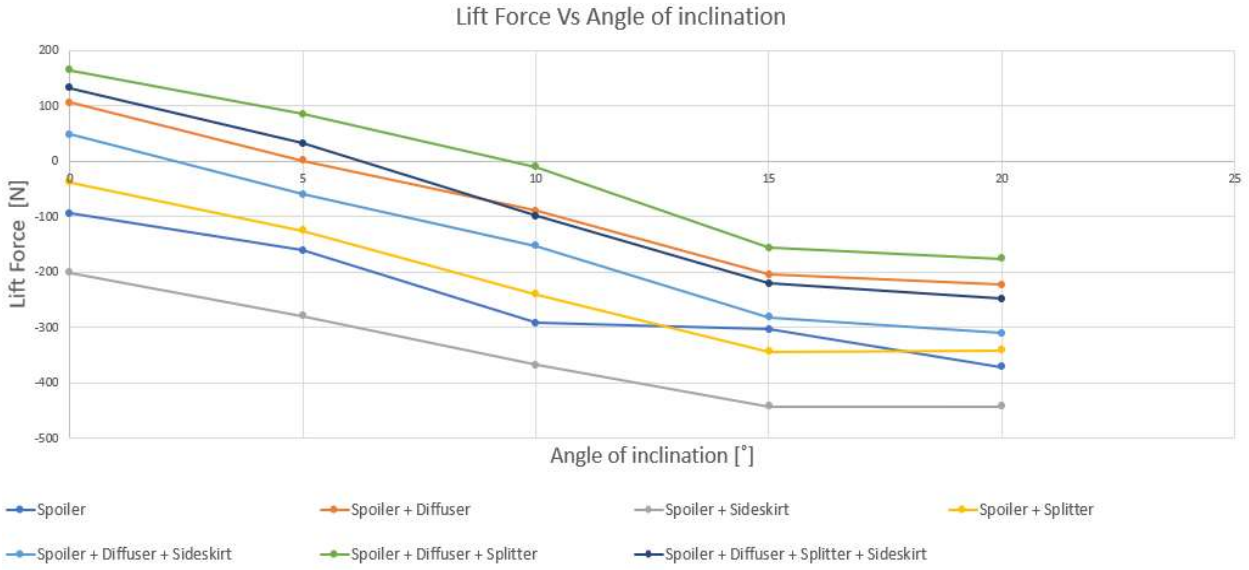

Fig. 50. Lift Force vs Angle of Spoiler Inclination

The graph in Fig.50, exhibits the seven configurations tested for lift force. The Y-axis represents the lift coefficient lift force and X-axis represents the angle of spoiler inclination. In this case the graph has a steady decrease, the reason being that as the downforce on each tested configuration increases the lift force decreases. This decrease in the lift force is considered as downforce and is tabulated and a graph has been plotted respectively. Each configuration has different values at the 5 different spoiler inclination angles tested. From the graph it is observed that the spoiler and side skirt configuration experiences maximum downforce because they have the least lift coefficient, and the spoiler, the diffuser, and the splitter configuration experience the least downforce for the simple reason that they have the maximum lift coefficient.

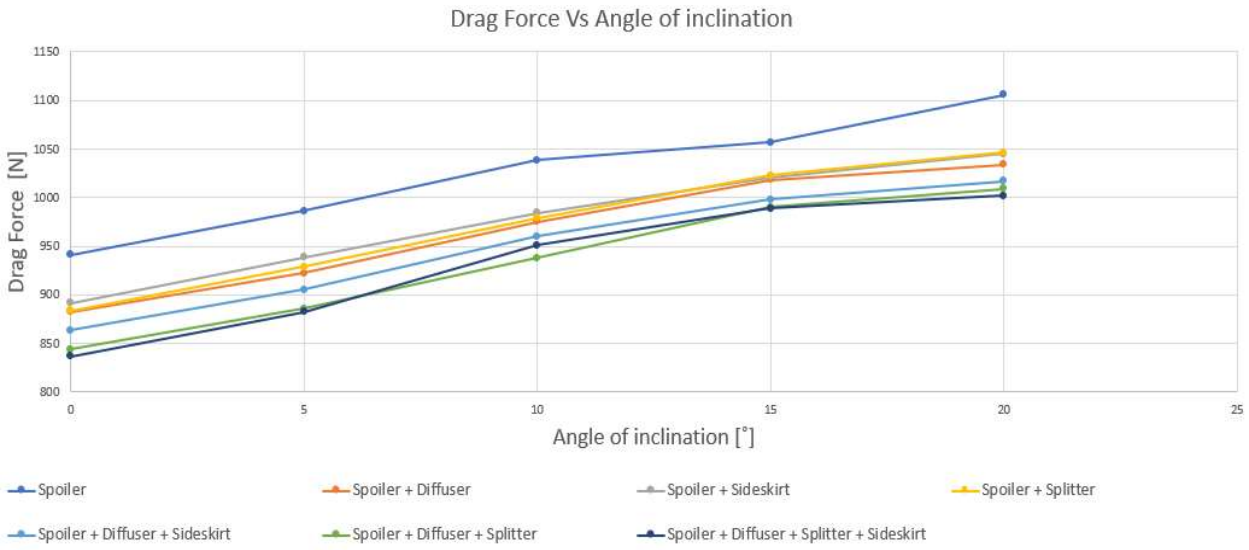

Fig. 51. Drag Force vs Angle of Spoiler Inclination

The graph in Fig.51 displays the seven configurations tested for drag force. The Y-axis represents the lift coefficient drag force and X-axis represents the angle of spoiler inclination. In this case the graph has a steady increase in drag force. This increase in the drag force is tabulated and a graph has been plotted respectively. Each configuration has different values at the 5 different spoiler inclination angles tested. From the graph it is observed that the spoiler configuration experiences maximum drag force because they have the highest drag coefficient, and the spoiler, the diffuser, the side skirt, and the splitter configuration experience the least drag force for the simple reason that they have the least drag coefficient.

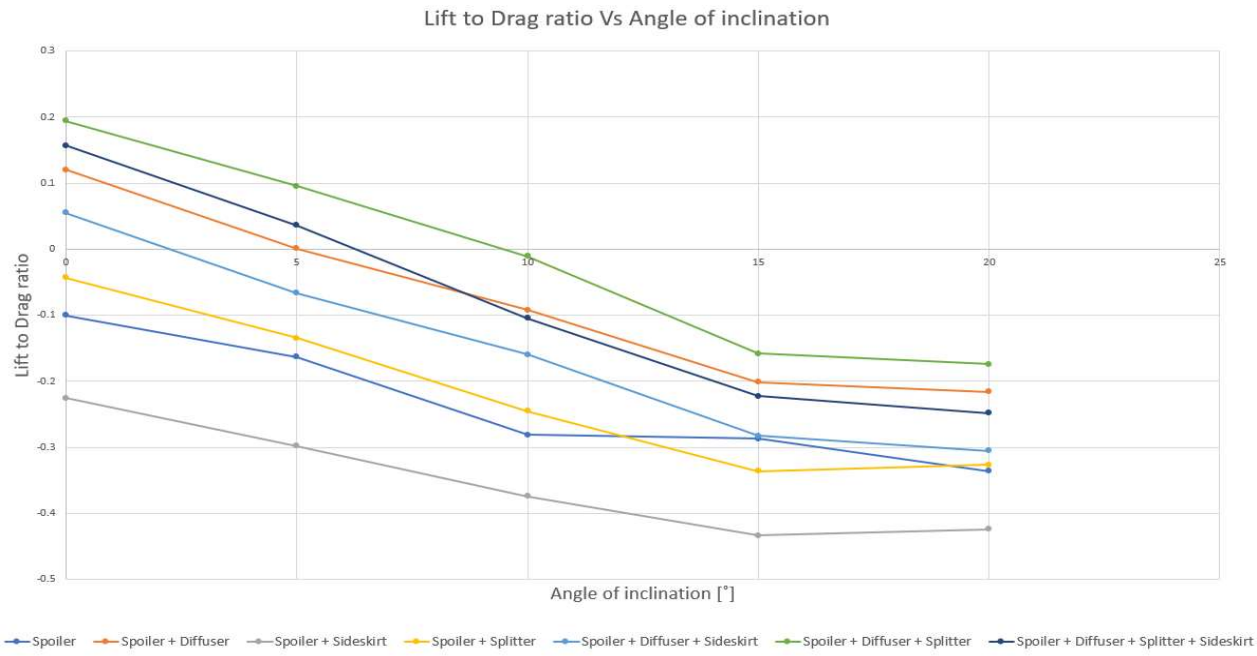

Fig. 52. Lift to Drag ratio vs Inclination angle

The graph above in Fig.52 indicates the Lift to Drag ratio vs Inclination angle for the all the configurations analyzed. The X-axis represents the angle of spoiler inclination and the Y-axis represents the lift to drag coefficient. This graph displays the average characteristics of lift coefficient and drag coefficient put together as a ratio. As seen from the graph, it has a steady decrease at first and stabilizes at an angle of 15˚. This angle of 15˚ is considered as the critical angle.

Pressure coefficients is a well-known parameter in the computation aerodynamics of the car, to study the compressibility and incompressibility of a fluid. It is a dimensionless quantity and is expressed as [35]:

$$Cp = \frac{(p - p_{ref})}{\frac{1}{2}\rho v^2}; \quad (3.1)$$

where:

p_{ref} – reference pressure

p – calculated mean pressure

v – velocity of the fluid

ρ – is the density of the fluid

Figures below show the pressure coefficient of stock car and all the configurations compared individually at the body centerline with the spoiler angle of 0˚, the diffuser angle 1˚ and the side skirt at a height of 205 mm with respect to the road surface. Pressure coefficient of the car is plotted along the car's longitudinal Z–axis for the respective top and bottom of the car. The trend of pressure coefficient distribution is consistent. *Cp* has a very small change from the bonnet to the rear windshield. However, a substantial variation of *Cp* begins from the start of the front bumper to the bonnet of the car. This signifies a region of high pressure experienced at the front end of the car along the effect of underbody structure is obvious on flow structure of body surface. At the rear end of the car the pressure coefficient is lower compared to the front end of the car, thus signifying that at the rear end the pressure is lower as the air flows from the rear wind screen to the ground surface. This is expressed for all the configurations of the car with slight variations in the pressure at the front end and at the rear end of the car.

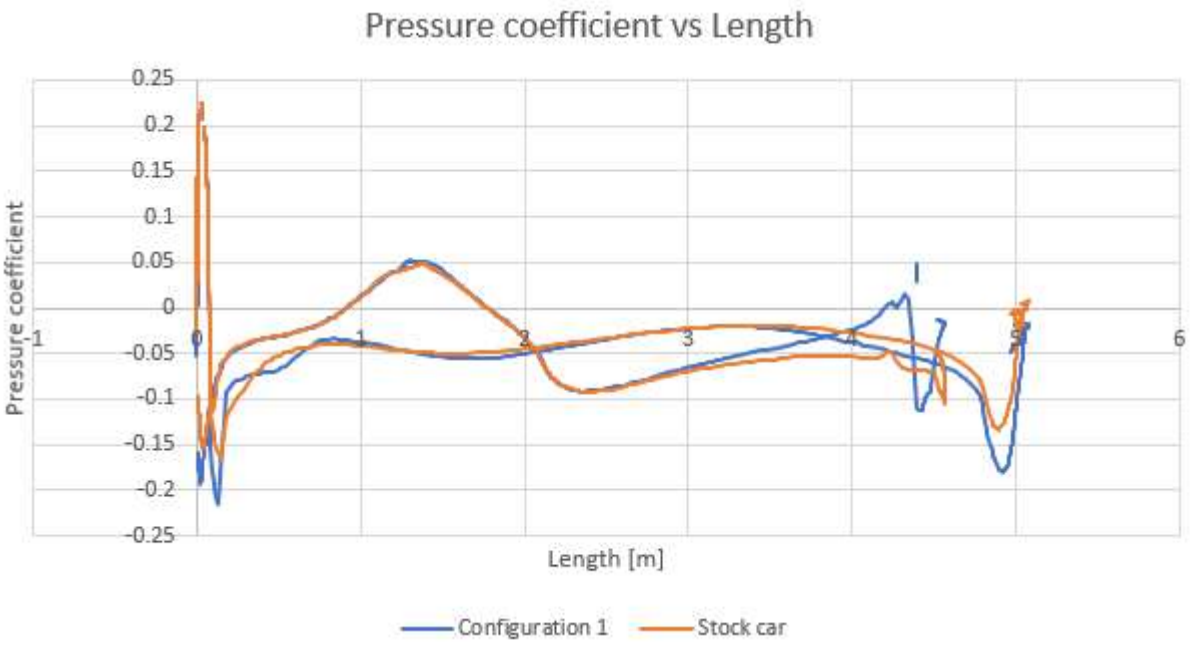

Fig. 53. Pressure coefficient of the stock car and configuration 1 along the length of the vehicle

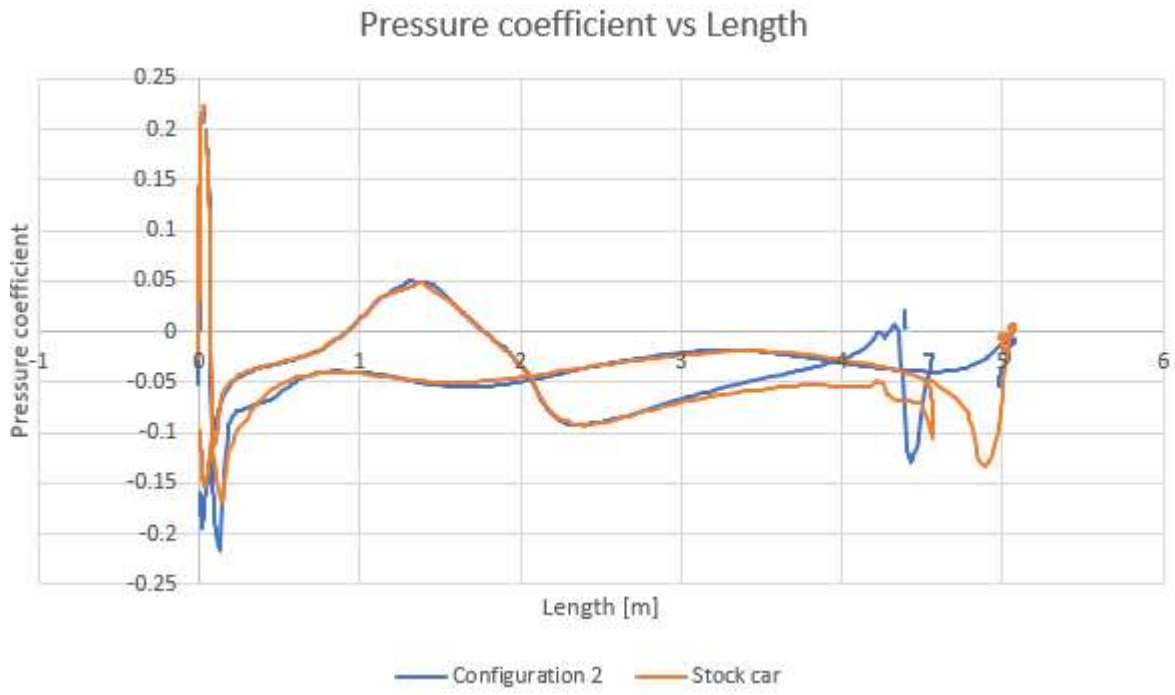

Fig. 54. Pressure coefficient of the stock car and configuration 2 along the length of the vehicle

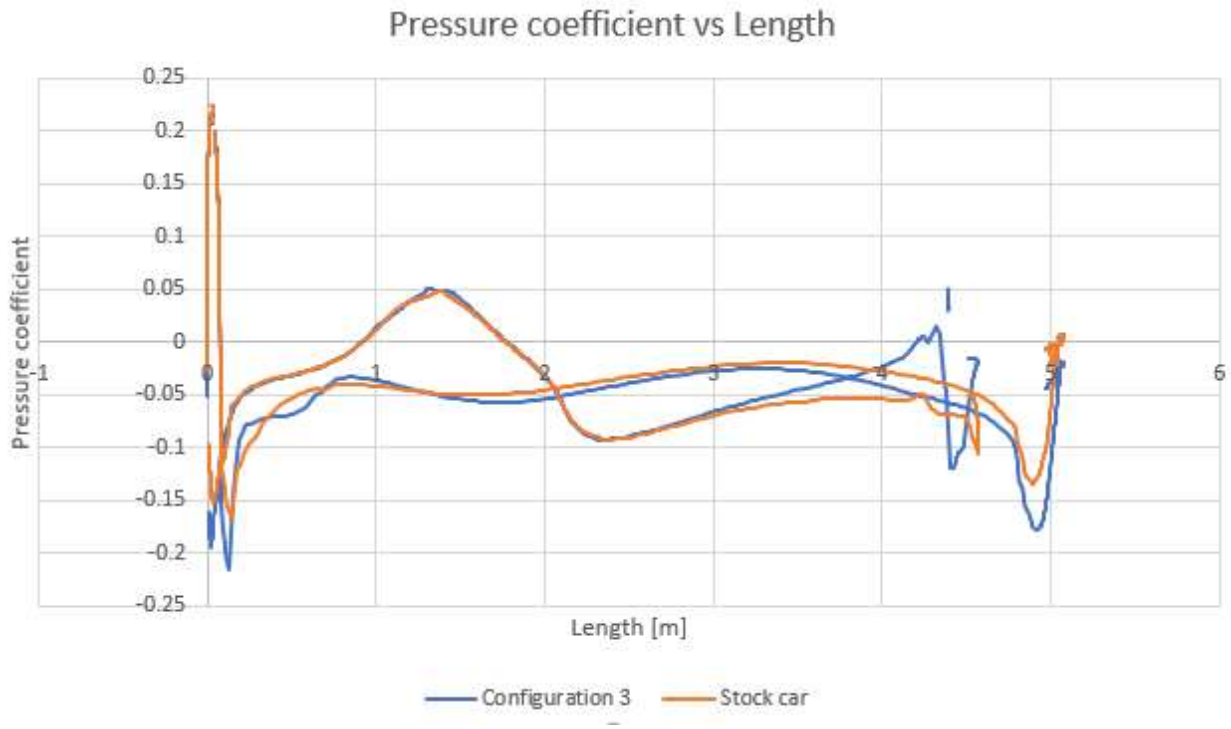

Fig. 55. Pressure coefficient of the stock car and configuration 3 along the length of the vehicle

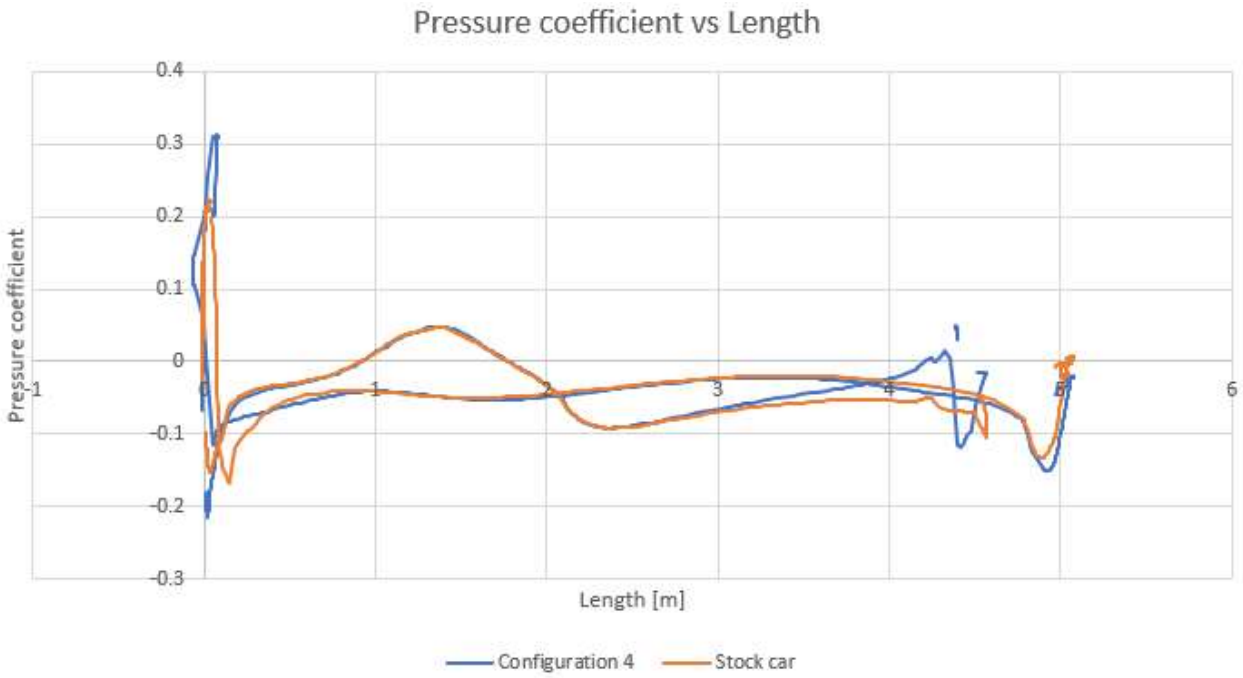

Fig. 56. Pressure coefficient of the stock car and configuration 4 along the length of the vehicle

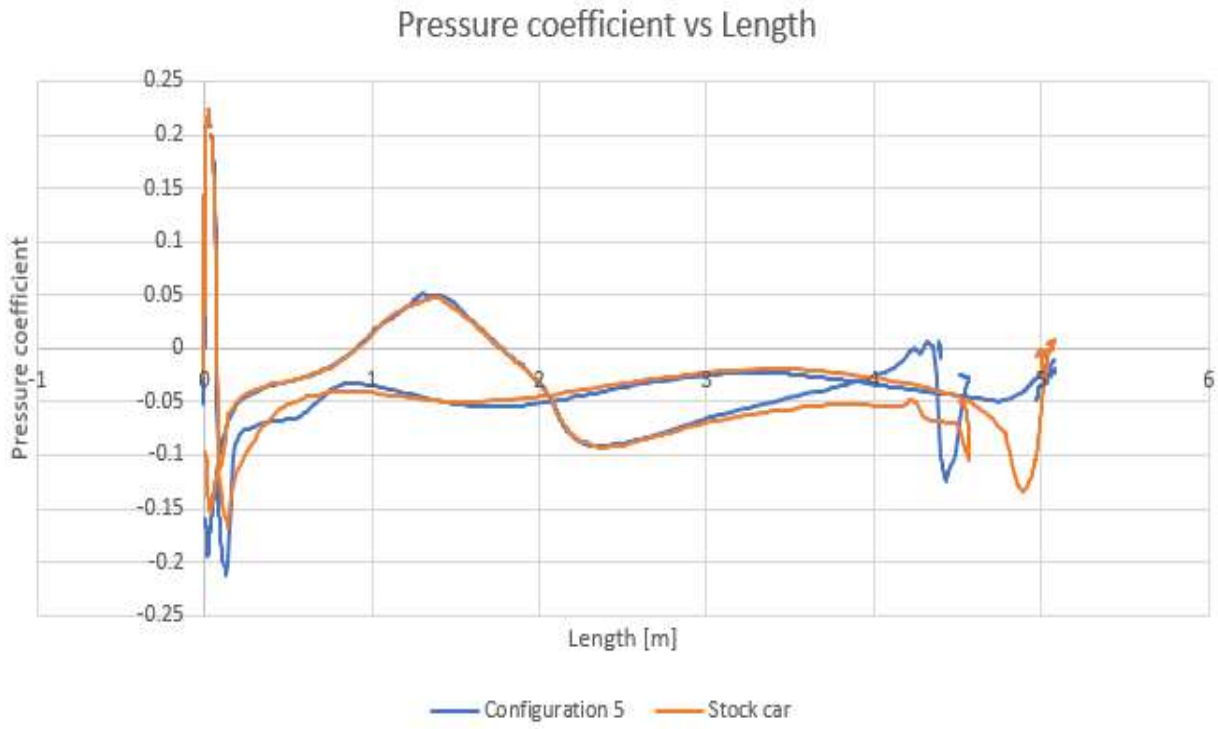

Fig. 57. Pressure coefficient of the stock car and configuration 5 along the length of the vehicle

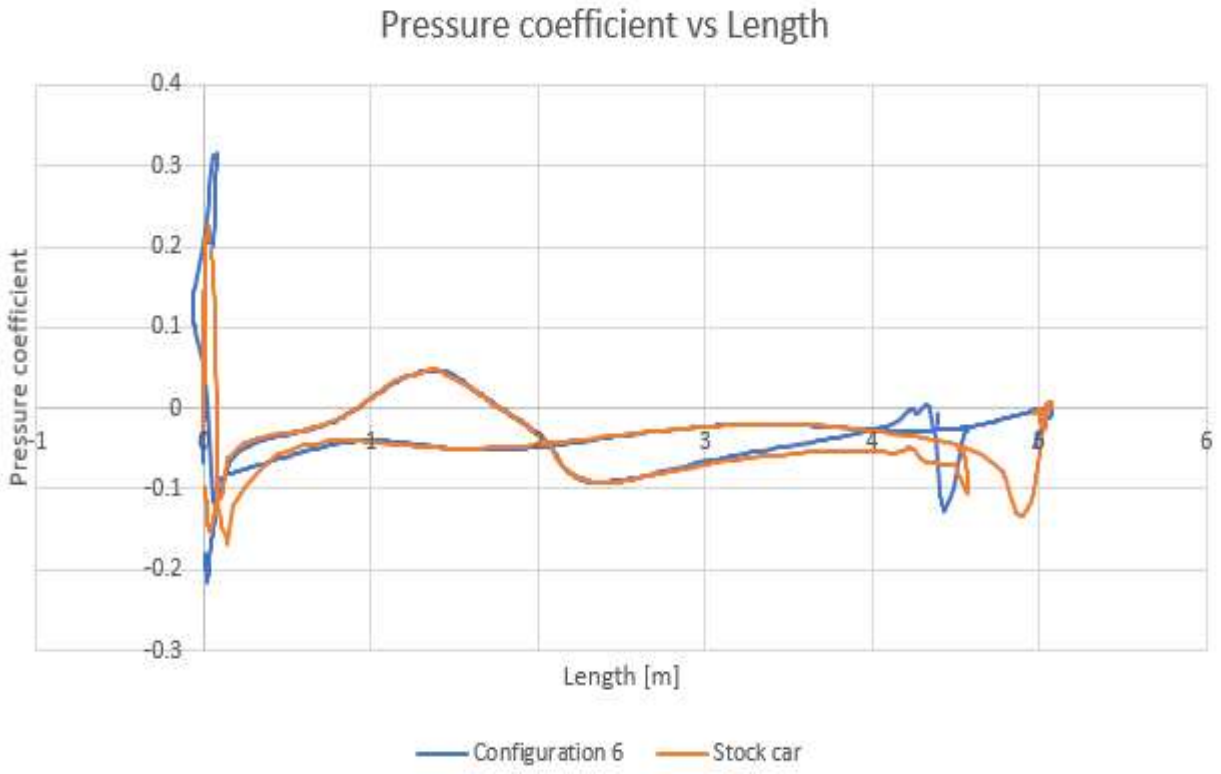

Fig. 58. Pressure coefficient of the stock car and configuration 6 along the length of the vehicle

3.11. Comparison

With all the required tests performed we tabulate the results of the seven configuration and compare with the stock car. The configuration with the least drag and lift coefficient is chosen. As seen, the Table.8 below compares all the seven configurations for the drag coefficient and drag force at different angles of spoiler inclination. From this table in configuration 7 experiences the least drag coefficient of 0.3607 and a drag force of 836.9 N. With lesser drag coefficient the drag force experienced by the vehicle is less hence better fuel efficiency.

Table 8. Comparison of drag attributes of the car at different configurations

Setup	Angles	Drag Coefficient	Drag Force	Least Drag coefficient	Least Drag Force
Configuration 1 - Spoiler	0	0.4055	940.9	0.4055	940.9
	5	0.425	986		
	10	0.4475	1038.3		
	15	0.4555	1056.7		
	20	0.4766	1105.8		
Configuration 2 - Spoiler + Diffuser	0	0.3803	882.4	0.3803	882.4
	5	0.3975	922.3		
	10	0.4203	975.1		
	15	0.4389	1018.2		
	20	0.4457	1034.0		
Configuration 3 - Spoiler + Side skirts	0	0.3843	891.7	0.3843	891.7
	5	0.4044	938.3		
	10	0.4243	984.5		
	15	0.44	1020.8		
	20	0.4505	1045.2		
Configuration 4 - Spoiler + Splitter	0	0.381	883.9	0.381	883.9
	5	0.4004	929.1		
	10	0.4219	978.9		
	15	0.4409	1023		
	20	0.4509	1046.1		
Configuration 5 - Spoiler + Diffuser + Side skirts	0	0.3723	863.8	0.3723	863.8
	5	0.3903	905.5		
	10	0.4138	960.1		
	15	0.4303	998.3		
	20	0.4384	1017.1		
Configuration 6 - Spoiler + Diffuser + Splitter	0	0.3638	844.1	0.3638	844.1
	5	0.3816	855.8		
	10	0.4042	937.9		
	15	0.4268	990.3		
	20	0.4349	1009		

Configuration 7 - Spoiler + Diffuser + Splitter + Side skirts	0	0.3607	836.9	0.3607	836.9
	5	0.3804	882.5		
	10	0.41	951.2		
	15	0.4262	988.9		
	20	0.4318	1001.7		

As perceived from the Table.9, with increase in Inclination angle, lift coefficient decreases, increasing downforce. But with greater angles of spoiler inclination the drag coefficient increases. Since the drag coefficient is smallest at the spoiler angle 0˚ for all the configurations, the least lift coefficient must also be considered with corresponding angle 0˚. The table below compares all the seven configurations for lift coefficient and lift force at different angles of spoiler inclination. From the Table.9 in configuration 3 that is spoiler and side skirt attached to the stock car experiences the least lift coefficient of -0.0867 and a lift force of -201.2. With this low lift coefficient, the downforce of the vehicle is increased yielding better stability, handling, and traction to the road surface.

Table 9. Comparison of lift attributes of the car at different configurations

Setup	Angles	Lift Coefficient	Lift Force	Least Lift coefficient	Least Lift Force
Configuration 1 - Spoiler	0	-0.0406	-94.4	-0.0406	-94.4
	5	-0.0694	-161.1		
	10	-0.1258	-291.9		
	15	-0.1307	-303.3		
	20	-0.1602	-371.6		
Configuration 2 - Spoiler + Diffuser	0	0.0457	106.1	0.0457	106.1
	5	0.0004	1.1		
	10	-0.0388	-90.1		
	15	-0.0883	-204.8		
	20	-0.0963	-223.5		
Configuration 3 - Spoiler + Side skirts	0	-0.0867	-201.2	-0.0867	-201.2
	5	-0.1204	-279.3		
	10	-0.1586	-368.1		
	15	-0.1907	-442.5		
	20	-0.1908	-442.7		
Configuration 4 - Spoiler + Splitter	0	-0.0165	-38.3	-0.0165	-38.3
	5	-0.0539	-125		
	10	-0.1035	-240.1		
	15	-0.1483	-344		
	20	-0.1472	-341.6		
Configuration 5 - Spoiler + Diffuser + Side skirts	0	0.0206	48	0.0206	48
	5	-0.0259	-60.1		
	10	-0.066	-153.2		
	15	-0.1216	-282.2		
	20	-0.1337	-310.2		

Configuration 6 - Spoiler + Diffuser + Splitter	0	0.0707	164.2	0.0707	164.2
	5	0.0365	84.8		
	10	-0.0045	-10.4		
	15	-0.0675	-156.6		
	20	-0.0758	-175.8		
Configuration 7 - Spoiler + Diffuser + Splitter + Side skirts	0	0.0566	131.6	0.0566	131.6
	5	0.0138	32		
	10	-0.0427	-99.1		
	15	-0.0949	-220.3		
	20	-0.1073	-249		

With the results of least drag coefficient and lift coefficient determined, we compare this with the base results of the car. But the drag coefficient of the car is least with configuration 7 and that of the lift coefficient is with configuration 3. The drag coefficient of the configuration 7 is lesser than configuration 3, whereas the lift coefficient is slightly greater. Since the aim is to improve the overall aerodynamic efficiency of the car, configuration 7 is most preferred.

The pressure coefficient of the stock car and configuration 7 are compared as shown in Fig.59. The pressure of configuration 7 in the interval 0 to 1 is initially high since there is addition of a splitter to the bottom of the front bumper. This increases the pressure faced at the front upper end of the car when compared to the stock car. Likewise, in the same interval, the pressure coefficient of the car is lowest for the configuration 7 due to splitter attached at the front as it pushes the air under the car at a greater velocity when compared to the stock car hence creating a region of low pressure underneath the car near the front bumper. The middle sector is similar for both the stock car and configuration 7. When noticed at the rear end in the interval 4 to 5, the coefficient for the configuration 7 is closer in length when compared to the stock as the diffuser attached plays a role in pressure reduction as it increases the velocity of air underneath the car.

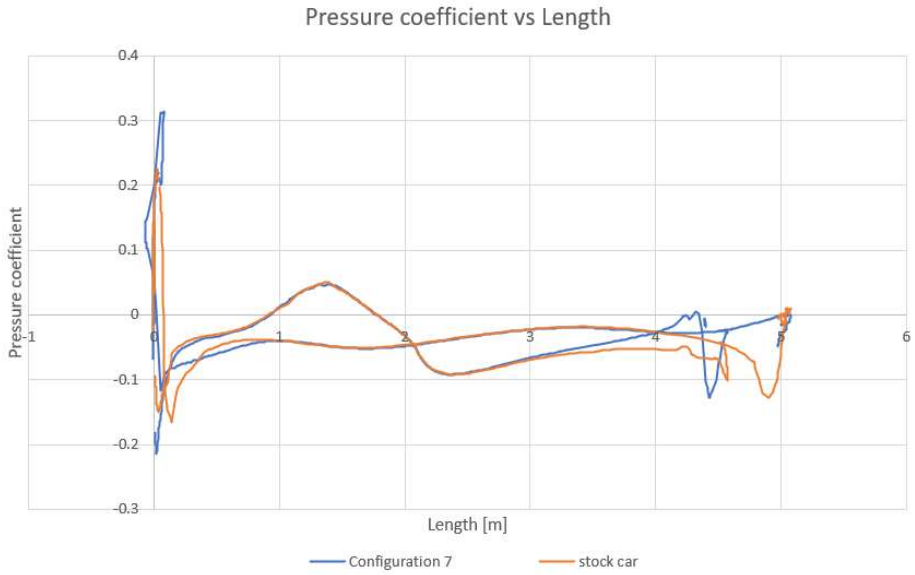

Fig. 59. Comparison of pressure coefficient between the stock car and configuration 7

Table 10. Comparison of the base results with results of configuration 7

Setup	Drag coefficient	Lift coefficient	Drag Force	Lift Force
Stock car	0.3793	0.2178	880.1	505.5
Configuration 7 (Spoiler, diffuser, splitter, side skirt)	0.3607	0.0566	836.9	131.6
Percentage Change	**4.90%**	**74.01%**	**4.91%**	**73.95%**

The drag coefficient of the car by the manufacture is 0.35 and the results of the stock car after CFD analysis is 0.3793. Since the difference percentage is 7.9%, we compare the results acquired. With this configuration, the drag coefficient of the car is lower by 4.9% when compared to the stock the fuel consumption is lesser. Correspondingly, with the decrease in lift coefficient, by 74% resulting in better downforce. Thus, providing better handling capabilities and improved traction.

Conclusion

1. Investigation on various streamlined aerodynamic features for a passenger car has been successfully assessed and reviewed. It is comprehensible from this review, using aerodynamic features an optimal design is to be made to attain a gain in performance of the car by reduction in drag coefficients and increase in downforce.
2. The Stock car and the aerodynamic features are successfully designed with Solidworks software with the necessary dimension to obtain a gain in performance as per requirement. The stock car designed was analysed at four different speeds and a drag coefficient of 0.3793, a drag force of 880.1 N, lift coefficient 0.2178 and lift force of 505.5 N were plotted. This result obtained was set as a baseline for comparison. The drag coefficient of the car by the manufacture is 0.35 and the results of the stock car after CFD analysis is 0.3793. Since the difference percentage is 7.9%, we compare the results acquired.
3. Analysis for the diffuser is performed at 4 different speeds for 5 different angles of the diffuser. Since the analysis for the configuration setup is performed at 40 m/s, we choose the same for the diffuser and side skirt. Angle 1˚ is chosen as the diffuser angle for the configuration setup as it offers better drag coefficient of 0.3771 and lift coefficient of 0.2163. Side skirt analysis was also performed at 4 different speeds for 5 different heights with respect to the ground surface. Height of 205 mm was selected as it displays least drag coefficient of 0.3428 and lift coefficients of 0.1825.
4. Different aerodynamic parts designed were assembled in the Solidworks assembly window and each aerodynamic feature was setup at different configurations and CFD analysis performed using Solidworks. The test was performed with a constant speed of 40 m/s and different spoiler inclination angles varying from 0 to 20 degrees. The results obtained are plotted in the form of a graph and are compared with each configuration. The drag coefficient vs angle of spoiler inclination has a steady increase while, the lift coefficient vs angle of spoiler inclination has a gradual decrease.
5. Configuration 7 is chosen out of the rest of the seven configurations for the reason being it has the least drag coefficient of 0.3607, a drag force of 836.9 N, and a comparably lower lift coefficient of 0.0566 and lift force of 131.6 N. The results of configuration 7 are compared with the results of the stock car and it is proven to provide better aerodynamic performance. Since the drag coefficient and drag force of the car is lower by 4.90% and 4.91% when compared to the stock car, the fuel consumption is lower. Correspondingly, with the decrease in lift coefficient and lift force by 74.01% and 73.95% respectively, resulting in better downforce. Thus, providing better handling capabilities and improved traction.

List of References

[1]. Ragavan, T et al. Aerodynamic Drag Reduction on Race Cars. s.l. : Journal of Basic and Applied Engineering Research, 2014. Vol. 1. 2350-0255.

[2]. Corno, matteo et al. Performance Assessment of Active Aerodynamic Surfaces for Comfort and Handling Optimization in Sport Cars. s.l. : IEEE, 2016. Vol. 24. 10636536

[3]. Dharmawan, mohammad arief et al. Aerodynamic analysis of formula student car. s.l. : AIP Conference Proceedings, 2018. Vol. 1931. 15517616.

[4]. Katz, joseph. Aerodynamics in motorsports. s.l. : Proceedings of the Institution of Mechanical Engineers, Part P: Journal of Sports Engineering and Technology, 2019. 1754338X.

[5]. Kumar, ravi B et al. Aerodynamic design optimization of an automobile car using computational fluid dynamics approach. s.l. : Taylor & Francis, 2019. 14484846.

[6]. Alkan, bugra. Aerodynamic Analysis of Rear Diffusers for a Passenger Car by Using CFD. s.l. : 7th International Advanced Technologies Symposium (IATS'13), 2019.

[7]. Katz, joseph. Aerodynamics of Race Cars. s.l. : Annual Review of Fluid Mechanics, 2006. Vol. 38. 0066-4189.

[8]. Durrer, simon. Aerodynamics of race car wings: A CFD study. 2016.

[9]. Basson, johan. Analysis of the aerodynamic attributes of motor vehicles. 2013.

[10]. Damjanovic, darko et al. CFD analysis of concept car in order to improve aerodynamics. s.l. : International Scientific and Expert Conference TEAM 2010, 2011. Vol. 1.

[11]. Ganesh Ayyar, eshaan. Wind-induced Stress Analysis of Front Bumper. s.l. : The International Journal Of Engineering And Science, 2016.

[12]. Hucho, W. H. sovran, G. Aerodynamics of road vehicles. 1993. 0408014229.

[13]. al, Samuel hellman et. Experimental Study comparing racecar aerodynamic downforce-generating devices using scale model nascar co. s.l. : International Journal of Automotive Technology, 2016. Vol. 17. DOI 10.1007/s12239−016−0028−7.

[14]. al, Pal .S et. aerodynamic analysis of a concept car model S. s.l. : International Conference on Mechanical Engineering and Renewable Energy, 2016. 289536918.

[15]. Yakkundi, vivek. mantha, S S. Effect of Spoilers on Aerodynamic Properties of Car Effect of Spoilers on aerodynamic properties of a car. s.l. : International Journal of Scientific Research and Review, 2018. Vol. 7. 2279-543X.

[16]. al, CHIEN-hsiung tsai et. Computational aero-acoustic analysis of a passenger car with a rear spoiler. s.l. : Applied Mathematical Modelling, 2009. Vol. 33. 0307904X.

[17]. al, Kurec Krzysztof et. International Journal of Mechanical Sciences. s.l. : International Journal of Mechanical Sciences, 2019. Vol. 152. 00207403.

[18]. Jacuzzi, eric. granlund, Kenneth. Passive flow control for drag reduction in vehicle platoons. s.l. : journal of Wind Engineering and Industrial Aerodynamics, 2019. Vol. 189. 01676105.

[19]. Chandra, S. CFD Analysis of PACE Formula-1 Car. s.l. : Computer-Aided Design and Applications, 2011. Vol. 8. 16864360.

[20]. Jameson, antony. Fatica, Massimilinnao. Using computational fluid dynamics for aerodynamics-a critical assessment. s.l. : Icas, 2002. 0962-7480.

[21]. Ansari, abdul razzaque. CFD analysis of aerodynamic design of Tata Indica car. s.l. : International Journal of Mechanical Engineering and Technology, 2017. Vol. 8. 0976-6340.

[22]. A, Asif ahmed. Cfd Analysis of Diffuser in a Car for Downforce Generation. s.l. : International Journal of Research in Engineering and Technology, 2016. Vol. 5. DOI: 10.15623/ijret.2016.0507026.

[23]. Ljungskog, emil et al. Inclusion of the physical wind tunnel in vehicle CFD simulations for improved prediction quality. s.l. : Journal of Wind Engineering and Industrial Aerodynamics, 2020. Vol. 197. 01676105.

[24]. HU, xingjun et al. Influence of different diffuser angle on Sedan's aerodynamic characteristics. s.l. : Physics Procedia, 2011. Vol. 22. 18753892.

[25]. Padagannavar, praveen. bheemanna, Manohara. Automotive computational fluid dynamics simulation of a car using ansys. s.l. : International Journal of Mechanical Engineering and Technology, 2016. Vol. 7. 0976-6340.

[26]. Das, rubel chandra. riyad, Mahmud. CFD analysis of passenger vehicleat various angle of rear end spoiler. s.l. : Procedia Engineering, 2017. Vol. 194. 18777058.

[27]. Kumar, Manoj et al. CFD Analysis of an Automobile to Improve the Aerodynamics. s.l. : International Journal Of Advance Scientific Research And Engineering Trends, 2017. Vol. 2. 2456-0774 .

[28]. Santos, rodrigo de oliveira et al. Aerodynamic Design of Super Efficient Vehicle. s.l. : SAE International, 2012.

[29]. Huminic A, Huminic G. CFD Investigations of an Open-Wheel Race Car. In4th European Automotive Simulation Conference, EASC 2009 Jul 6 (pp. 85-94).

[30]. Padagannavar P, Bheemanna M. Automotive computational fluid dynamics simulation of a car using Ansys. International Journal of Mechanical Engineering and Technology (IJMET) Volume. 2016
[31]. Yuan Z, Wang Y. Effect of underbody structure on aerodynamic drag and optimization. Journal of Measurements in Engineering. 2017
[32]. Ljungskog E, Sebben S, Broniewicz A. Inclusion of the physical wind tunnel in vehicle CFD simulations for improved prediction quality. Journal of Wind Engineering and Industrial Aerodynamics. 2020 Feb
[33]. Chandra S, Lee A, Gorrell S, Jensen CG. CFD analysis of pace formula-1 car. Computer-Aided Design & Applications, PACE (1)
[34]. Boretti A. Analysis of lift and drag coefficients of a GT2 racing car at various speeds with movable wheels and ground. World Journal of Engineering. 2015
[35]. Yuan Z, Gu Z, Wang Y, Huang X. Numerical investigation for the influence of the car underbody on aerodynamic force and flow structure evolution in crosswind. Advances in Mechanical Engineering. 2018
[36]. Matsson JE. An Introduction to SolidWorks Flow Simulation 2013. SDC publications; 2013.
[37]. Sobachkin A, Dumnov G. Numerical basis of CAD-embedded CFD. InNAFEMS World Congress 2013